1. Introduction

1.1. General problems in development of cancer treatment even after 50 years of endeavor

Cancer remains the major cause of death in most advanced countries in the world, and the incidence of cancer increases as populations age. The best treatment of malignancies such as gastric, colonic, and cervical cancers is surgical removal of early-stage tumors that are small and confined to a limited area, without metastasis. Chemotherapy, and to a limited extent radiotherapy, have been the last resort to control cancer. However, conventional chemotherapy, which utilizes small molecular drugs, is far from successful, similar to the situation that we have experienced with antibiotics given for microbial infections. This problem derives mostly from the lack of tumor selectivity, or so-called selective toxicity, of these agents, so that severe adverse effects limit usage. Thus, an urgent need exists to develop drugs with high selectivity to target tumors, which may greatly reduce drug toxicity and enhance the therapeutic efficacy of chemotherapeutics.

Another so far unsuccessful direction of recent cancer treatment is so-called molecular target therapy, which usually focuses on specific kinases or receptors that are overexpressed in cancer cells or tissues. Recent clinical results for those molecular target drugs have been disappointing [1–3]. The benefit for patients undergoing these treatments is a 1–2 month extension of the usual 3- to 5-year overall survival [1,3]. In another study, a combination of two different types of molecular target drugs resulted in shorter overall survival [2]. Adverse side effects were not easily overcome, and the frequency of medical emergencies was not reduced. Among these drugs, one exception was imatinib (Gleevec), which is used for chronic myelogenous leukemia. However, most cases demonstrated drug resistance after several months of its use. The problems associated with molecular target drugs probably relate to the intrinsic genetic diversity of human solid tumors, which these drugs do not account for [4,5]. Usually, multiple genes or their product proteins, which make up sophisticated networks, support or promote the growth, cell regulation, invasion and metastasis of tumor cells. These genes are now known to undergo extensive mutations. Findings for 11 patients with breast cancer and 11 patients with colorectal cancer showed that individual tumors demonstrated an average of approximately 90 mutated genes, and 189 genes mutated at a significantly high frequency [5]. These data mean that the patients had only a small (few percent) chance of the likelihood of a positive response to the molecular target drugs. In addition to the high frequency of occurrence of mutant genes, redundant genetic and molecular or metabolic pathways, which constitute the backup system of vital molecular pathways, may invalidate the single gene or receptor concept and single pathway assumption. Thus, such a highly specific molecular approach, targeted to even a single epitopic antigen, receptor, or kinase, seems to be an imperfect if not an unwise approach.

Another problem may reside in the *in vitro* screening method for cancer chemotherapeutics. This method utilizes the individual cancer cell type panel model, and a drug is thus screened on the basis of tumor cell type. However, even after more than 30 years of screening at least 50 cell types, such as glioblastoma, malignant melanoma, hepatoma, pancreatic cancer and cervical cancer, no revolutionary discovery of new useful drugs has been reported. One problem with this screening system is probably related to a lack of considering pharmacokinetics and the vascular phenomenon named the *enhanced permeability and retention* (EPR) effect, so that only cytotoxic compounds were identified.

1.2. The EPR effect: the cutting edge

The greatest breakthrough leading to more general targeted antitumor therapy was the discovery of the EPR effect, as commented by Torchilin [6], (in this issue of ADDR).

The EPR effect was first reported by Matsumura and Maeda in 1986 [7] and was described in greater detail and validated by Maeda et al. [8–14]. Their investigations showed that most solid tumors have blood vessels with defective architecture and usually produce extensive amounts of various vascular permeability factors. Most solid tumors therefore exhibit enhanced vascular permeability, which will ensure a sufficient supply of nutrients and oxygen to tumor tissues for rapid growth. The EPR effect considers this unique anatomical–pathophysiological nature of tumor blood vessels that facilitates transport of macromolecules into tumor tissues. Macromolecules larger than 40 kDa selectively leak out from tumor vessels and accumulate in tumor tissues. In contrast, this EPR effect-driven drug delivery does not occur in normal tissues [7–14]. This unique phenomenon in solid tumors—the EPR effect—is thus considered to be a landmark principle in tumor-targeting chemotherapy and is becoming an increasingly promising paradigm for anticancer drug development. For example, Doxil, which is a PEGylated (polyethylene glycol-coated) liposome-encapsulated formulation of doxorubicin, was approved for treatment of Kaposi sarcoma and other cancers. Many other polymeric or micellar drugs are in clinical stage development (phases I and II) [15,16], of which only a few are reviewed in this special issue. Compared with conventional anticancer drugs, most of which are small molecular drugs, these macromolecular drugs have superior *in vivo* pharmacokinetics (e.g., a prolonged plasma half-life) and, more important, greater tumor selectivity, so that they produce improved antitumor effects with no or less adverse reactions [15–17].

The EPR effect has thus now become the "gold standard" in anticancer drug design and anticancer strategies using macromolecular agents, including gene delivery, molecular imaging, antibody therapy, micelles, liposomes, and protein–polymer conjugates (see Torchilin [6] in this issue of ADDR). As evidence of this status, the numbers of citations related to the EPR effect have been progressively increasing in recent years (Fig. 1).

1.3. Problems related to the EPR effect and their solutions

Regardless of the popularity of EPR effect-based drug delivery, many problems with that strategy still exist. We know that large tumors show great pathophysiological heterogeneity. Although we have identified many factors that affect vascular permeability in tumors, as described in the later sections of this article, some parts of

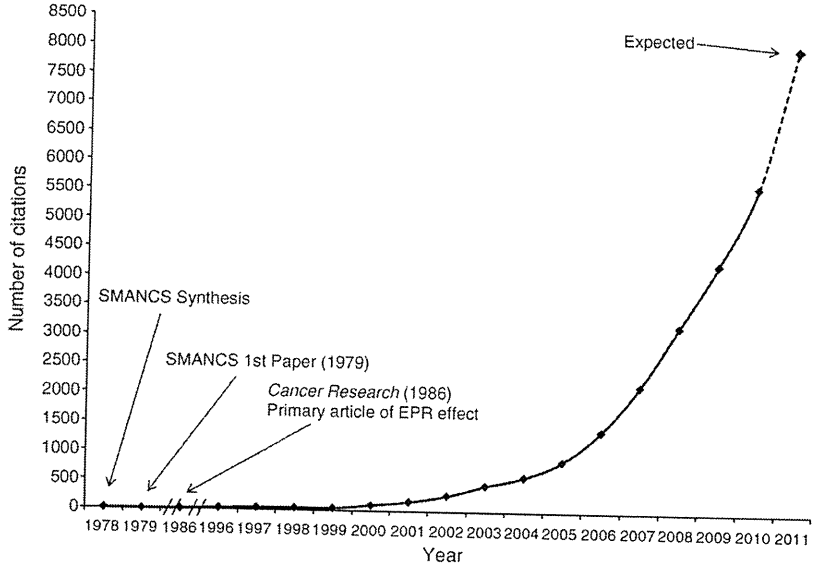

Fig. 1. Number of citations on the EPR effect.
Data are collected from the database of Science Direct, SciFinder and Web of Science.

tumors, particularly the central area of metastatic cancers, do not exhibit the EPR effect and show less accumulation of macromolecules than other parts [18,19]. Most of the *in vivo* experimental studies used mouse tumors that were usually 0.5–1 cm in diameter at least; larger tumors (e.g., 1–2 cm in diameter) tend to contain more necrotic tissues or highly hypovascular areas (with thus less chance of vascular leakage and less tumor growth because of the lack of blood vessels).

In an effort to solve some of these problems, we recently developed methods to intensify the EPR effect and to achieve a more homogeneous drug delivery to tumors, either by elevating blood pressure or by applying nitric oxide (NO)-releasing agents, as described later. The former method utilizes hydrodynamic enhancement of drug delivery; the latter is via generation of NO in tumor tissues. These developments allow one to envision improved cancer chemotherapy via macromolecular drugs in clinical situations.

This review summarizes and discusses the principle of the EPR effect, especially factors influencing this effect, its limitations and methods of avoiding such limitations. In addition, augmenting the EPR effect (tumor drug delivery) and reducing the heterogeneous consequences of the EPR effect to improve clinical outcome are also discussed.

2. The EPR effect: history and principle

In 1979, Maeda et al. [20] reported the first synthesis of the anticancer protein neocarzinostatin (NCS) conjugated with a polymer (styrene maleic acid copolymer, SMA), which named SMANCS. Later studies found SMANCS to accumulate to a greater degree than NCS in tumor tissues [7–14,21,22]. In addition, this biocompatible polymer conjugation of the protein prolonged the plasma half-life, often up to 200 times longer compared with unmodified free NCS or low-molecular-weight drugs [7,20–22]. Furthermore, this unique and important phenomenon was demonstrated with other plasma proteins of different molecular sizes. Proteins larger than 40 kDa showed selective accumulation in tumor tissues, to a degree far more than that observed in normal tissues, and these proteins were retained in tumor tissues for long periods: at 24 h after intravenous (i.v.) injection, the accumulation of most polymeric macromolecular drugs in tumor tissues was more than 10–200 times higher than that in normal tissues and organs, such as skin, muscle, heart, and kidney [7,9,10,15–17,23–28]. These findings led to generalization of the concept of the EPR effect. SMANCS, which took the advantage of the EPR effect, became the first macromolecular anticancer drug approved for use in clinical settings in 1993.

A typical experiment that illustrates the EPR effect involves using an i.v. injection of the dye Evans blue, which binds to plasma albumin and behaves *in vivo* like a true macromolecule, i.e., a putative macromolecular drug. Fig. 2A shows that 24 h after i.v. injection of Evans blue/albumin complex, the blue dye was seen in certain tumor sites, but normal tissues (e.g., skin) showed no blue staining. Moreover, in experimentally induced tumors larger than 3 cm in diameter, the blue dye was found primarily in the tumor periphery, where tumor growth and angiogenesis predominate (Fig. 2B). Frequently, as mentioned earlier, central regions of tumors are partly necrotic or hypovascular, so that area demonstrated no significant accumulation of blue dye (Fig. 2B). These findings suggested that the EPR effect (accumulation of macromolecular drugs) is a blood vessel-dependent phenomenon, which is discussed below in detail. Also, for example, in cancer patients, when hepatoma patients received intraarterial (i.a.) SMANCS in Lipiodol (i.e., a formulation of SMANCS with the lipid contrast agent), imaging of tumor-selective drug delivery became possible by use of computed tomography (CT). CT showed Lipiodol retention as high-density staining (Fig. 2C). The tumor/blood ratio of drug distribution had increased more than 2000 times, and that retention of Lipiodol could last for more than 2–3 months [27–31]. This tumor-selective delivery of SMANCS consequently led to a markedly regressed tumor (Fig. 2D), as well as prolonged survival of patients, without serious adverse side effects [18,19,29–31].

2.1. The EPR effect: a molecular size-based phenomenon

As mentioned above, the EPR effect is a molecular weight-dependent phenomenon: molecules or particles larger than 40 kDa, which is the threshold of renal clearance, showed a prolonged circulation time (thus, a much increased $t_{1/2}$) and hence very slow clearance from the body, with a higher AUC (area under the concentration–time curve) (Fig. 3). These molecules thus gradually permeated tumors in a selective fashion. In addition, these accumulated macromolecular drugs remained in tumors for a relatively long time (e.g., several days) [7–14]. The EPR effect was observed not only with proteins including immunoglobulin G (IgG), but also with drug–polymer conjugates, micelles, liposomes,

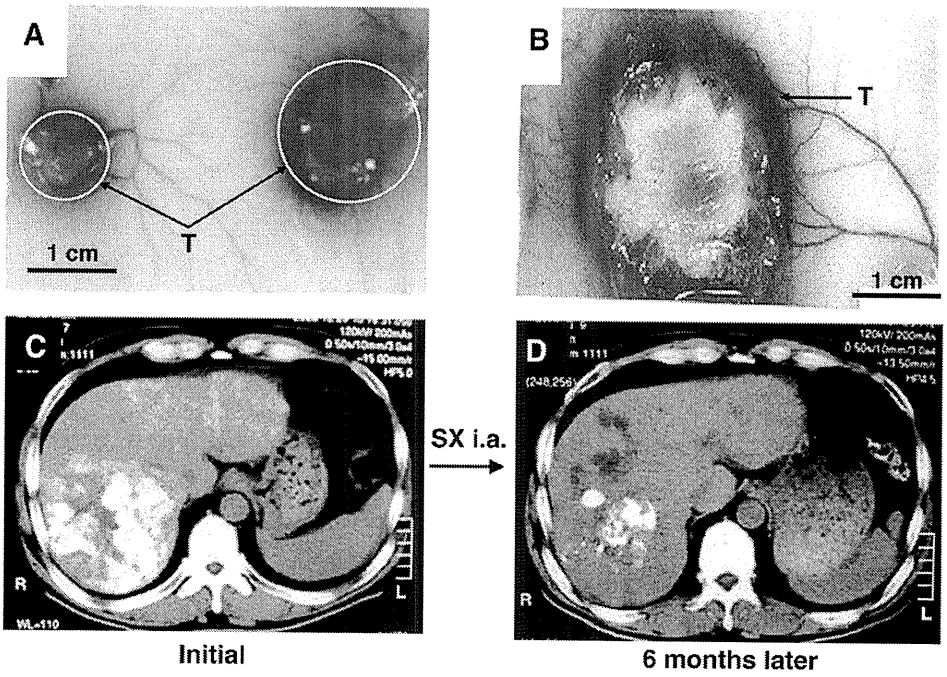

Fig. 2. Experiments illustrating the EPR effect. The EPR effect is shown by the putative macromolecular drug Evans blue/albumin complex (A, B), and by tumor-selective accumulation of the macromolecular anticancer drug SMANCS dissolved in Lipiodol (C, D). (A and B) Macroscopic images of tumor implanted in the skin of mice, at 24 h after i.v. injection of Evans blue (10 mg/kg). The tumor, *T* (circles and arrows), became progressively blue after injection. Normal tissue had no blue color. However, the tumor periphery (outside the circles in A) showed slight extravasation, which is thought to be the result of vascular mediators that diffused out of the tumor tissues and demonstrates the vascular permeability in the vicinity of the tumor, as discussed in elsewhere. (C and D) Computed tomography (CT) of a massive hepatocellular carcinoma after administration of SMANCS (SX)/Lipiodol (LP) given via the hepatic artery. Image was taken 2 days after the initial SX/LP injection, with the white areas in the right lobe (R) indicating tumor-selective uptake of the drug (C). After 3 injections of SX/LP in 6 months, tumor size was markedly reduced (D). The drug selectively retained in the tumor for a long time. R and L indicate right and left sides of the patient, respectively.
C and D are modified from Ref. [29] with permission.

nanoparticles of poly(lactic-co-glycolic acid) (PLGA), DNA polyplexes and lipid particles [7–14,32]. We initially examined *N*-(2-hydroxypropyl)methacrylamide (HPMA) copolymer, with a molecular size up to 778 kDa [33] and α_2-macroglobulin (α_2-M) (720 kDa) [20], both of which exhibited the EPR effect. Moreover, earlier work using *Lactobacillus* sp. and a more recent study using *Salmonella typhimurium* suggested that the EPR effect functions even for bacteria larger than 1000 nm [34–36].

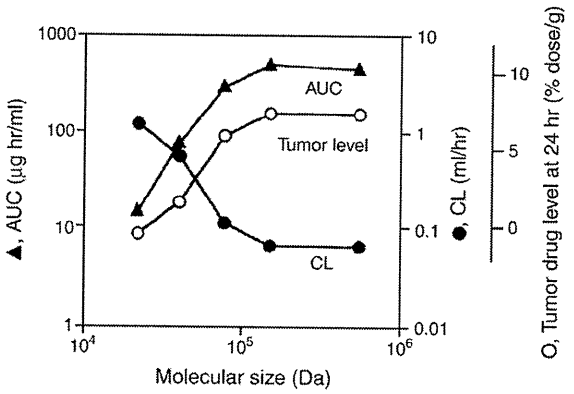

Fig. 3. Relationship of the molecular size of drugs to plasma drug concentration (AUC), renal drug clearance (CL) and intratumor drug uptake (as expressed by a percentage of injected dose). Mice received i.v. injections of putative polymeric drugs, which are ^{125}I-labeled Tyr-HPMA-copolymers of various molecular sizes, at 1.8×10^6 cpm per mouse. The tumor model was S-180. At various times (up to 24 h) after drug administration, mice were killed, and organs, tissues including blood and tumors were collected for counting of radioactivity, to estimate the drug distribution.
From Ref. [33] with permission.

However, the *in vivo* behavior of macromolecules, especially proteins, is one concern. Most proteins, when they are denatured, are of non-self origin, or are less biocompatible, can be cleared rapidly from the circulation via scavenger receptors or other mechanisms. For example, an asialoglycoprotein receptor of liver cells (parenchymal hepatocytes) rapidly cleared desialylated serum glycoproteins from the circulation [22]. Xanthine oxidase (XO) that is a 298-kDa molecule, is rapidly taken up by vascular endothelial cells after i.v. injection because of its high binding affinity to sulfated glycosaminoglycans on the endothelial cell surface; thus, no significant tumor uptake occurred in a mouse tumor model [37]. However, after PEGylation of XO, which involved masking the ε-amino groups of the lysine residues of XO that play a critical role in binding XO to vascular endothelial cells, tumors showed markedly increased drug (PEG-XO) accumulation, and thereby a marked antitumor effect was achieved [37]. Also, modifications or conformational changes of proteins may greatly affect their *in vivo* half-lives. One example involves α_2-M, a multifunctional protease inhibitor in plasma. In the normal state, native α_2-M has a plasma half-life of 140 h in mice. However, the plasma half-life of a α_2-M-plasmin complex decreased dramatically to only 5 min [22]. Thus, molecular weight is not necessarily the key determinant for attaining a long plasma half-life and a functional EPR effect. Biocompatibility in the broad sense is the key.

2.2. Problems and warnings during macromolecular drug development based on the EPR effect

As just stated, molecular weight is not the sole determinant of the EPR effect; other factors such as the surface charge and an *in vivo*

surveillance system for macromolecules (i.e., scavenger receptors of the reticuloendothelial system, RES) are quite important. The vascular endothelial luminal surface is known to carry a negative charge, so basic proteins with positive charges or cationic polymers rapidly bind to vascular endothelial cells, which results in a lower AUC, shorter plasma $t_{1/2}$, and a consequently reduced tumor drug accumulation by means of the EPR effect [38,39].

Acidic or neutral particles are thus expected to have a longer plasma half-life. However, the RES in the liver and spleen reportedly showed faster uptake of negatively charged nanoparticles and liposomes than that of neutral particles [40]. Nevertheless, α_1-acid glycoprotein with a pI of about 3.5 exhibited a long plasma half-life (e.g., 19 h for human α_1-acid glycoprotein in the rat; Ref. [41]). Also, in our previous work, we found that the acidic polymer-conjugated proteins SMANCS (pI of ~3.0) and serum albumin (pI of 4.8) showed long plasma half-lives and high tumor concentrations, although accumulation of SMANCS in the liver was also high [7,22]. These findings suggest that a surface charge may not cause all polymeric drugs and proteins to behave in the same way. Generalization on the basis of these data may therefore be difficult.

The RES, which demonstrates a rich presence in the liver and spleen, can be a major obstacle to tumor delivery of macromolecular drugs, as observed with liposomes in the 1960s to early 1970s [42]. To prevent phagocytic clearance by the RES, the most commonly used strategy is to conjugate PEG onto the surface of proteins or nanoparticles. The result is known as a stealth particle or liposome [42–44], which contains a hydrated water barrier that provides good steric hindrance to the attachment of phagocytes. PEGylation therefore reduces the rate of RES uptake and increases the circulation half-life of various types of nanoparticles, including liposomes [43,44], polymer-based nanoparticles [45] and hybrid nanoparticles [46]. PEGylation thus benefits EPR-based targeting of drugs to tumors.

However, it has been reported that injection of PEGylated liposomes will elicit PEG-specific IgM, thus inducing rapid elimination and enhanced hepatic uptake of a second dose of PEGylated liposomes, which is known as accelerated blood clearance phenomenon and is becoming a barrier to the pharmacokinetics and pharmacodynamics (PK/PD) of PEGylated liposomes and particles [47,48]. Investigations regarding this point are therefore necessary and will greatly improve the therapeutic efficacy of PEGylated drugs. In addition, certain PEG-modified macromolecules and particles are also now understood to have a slower uptake into tumor cells than non-PEGylated molecules [49]. This finding is believed to be one barrier against efficient drug delivery to tumor cells; this situation has been named the PEG dilemma [49]. Nevertheless, suppressed cellular uptake, perhaps a common characteristic of most PEGylated drugs, constitutes an important effect for achieving a longer plasma half-life. Therefore, avoidance of the PEG dilemma in targeted tissues (e.g., tumor) is becoming a critical issue. Developing suitable PEGylation strategies to achieve a longer plasma half-life, as well as better intracellular trafficking, is important. For example, one option may be using bonds that could be eventually cleaved by proteases or similar agents near tumor cells [49,50]. A different approach to avoiding the PEG dilemma may involve, as another example, using SMA conjugation or SMA micelles, in which the hydrophobic component of SMA would confer a higher affinity for cell membranes and improve endocytotic uptake in significant extent [51].

2.3. Problems unrelated to EPR effect: various barriers to drug delivery to target tumor tissues

Walls of blood vessels are the first barrier to drug delivery to target tumor tissues. However, according to the mechanism of the EPR effect, macromolecular drugs could easily reach the interstitium of tumor tissues from leaky tumor blood vessels. Vascular walls in tumors thus do not serve as a barrier for macromolecular drugs or nanomedicines; instead, they facilitate selective delivery of macromolecular drugs to tumor tissues.

The second barrier to successful delivery of macromolecular drugs to tumor cells is the requirement to cross matrix tissue surrounding target cells and target molecules in cells. Many tumor tissues are surrounded by coagulation-derived matrix gel such as fibrin gel or stromal tissues or are nodules encapsulated by fibroblasts. For these tumor tissues, release of low-molecular-weight drugs or cleavage from chains of polymer (e.g., PEG, as discussed above) and disintegration of micelles and liposomes may be an essential point. Moreover, macromolecules themselves can diffuse across matrix tissue for a considerable distance: for instance, IgG (160 kDa) can freely diffuse across 5 mm overnight in 1% agar gel. This second barrier may therefore not be such a serious problem for delivery of macromolecular drugs to tumors.

The third barrier to reaching target molecules is the cell membrane. For example, as described above for the PEG dilemma, PEG-coated macromolecules have a hydrated barrier on the surface that would resist endocytic uptake [49]. The use of short PEG (e.g., Mw<1000) or insertion of protease sensitive peptide between PEG and macromolecules (as described above) may be effective strategies to overcome the PEG dilemma [49,50]. Under these circumstances, an efficient internalization mechanism or transporter system is often better than simple free diffusion. Receptor-mediated endocytosis is thus expected to be an effective means to deliver macromolecular therapeutic agents into tumor cells. One such method uses conjugation of transferrin as a ligand because the transferrin receptor is significantly upregulated in many, if not all, malignant cells [52]. Nanoparticles with their surface modified with transferrin showed a markedly increased tumor-targeting property and intracellular uptake [53,54]. These points are also discussed in this special issue by Harashima and Maruyama.

Utilization of a transport system of cells such as the ATP-binding cassette (ABC) transporter would also be better than free diffusion of drugs. For instance, pirarubicin, which is a pyranyl derivative of doxorubicin, has a 3- to 4-fold faster cellular uptake than doxorubicin (another anthracycline), perhaps because it can utilize the glucose (pyranose) transport system. Pirarubicin micelles are thus advantageous because once the drug is released into the area around tumor cells, free pirarubicin is rapidly—more rapidly than doxorubicin—taken up by the cells [26,27].

The fourth barrier to effective macromolecular anticancer therapy is the release rate of the active principle of the drug from liposomes, micelles, or drug–polymer conjugates. The EPR effect will drive the macromolecules into tumor tissue. Nevertheless, the ultimate goal is access of active drugs to target sites. Therefore, the release rate at the target must be optimal (e.g., 3–10% per day), because too slow a release results in insufficient concentrations of active drugs at sites of action. Release that is too rapid would lead to a high concentration of free drug in circulation but no drug accumulation in the tumor, the results thus being a considerably lower therapeutic effect and undesired systemic toxicity. Micellar drugs that have a very rapid drug release (a micelle burst) after injection, e.g., 50% release within about ~30 min for several drugs, often demonstrate no EPR effect and an unsuccessful therapeutic effect. Liposomes are prepared to have adequate stability in solution (or an adequate shelf life) due to their cholesterol-enriched harder lamellar structure, so their rate of drug release could become too slow. Thus, micelles or liposomes with too stable an encapsulation construct, or too labile a composition, have *in vivo* pharmacological properties that make them unfit for clinical use, even though their *in vitro* data are excellent. Therefore, the optimal kinetics of drug release should be studied *in vivo* because cell-free *in vitro* systems may not accurately reflect *in vivo* conditions.

Similarly important is release of drugs from prodrugs or drug–polymer conjugates via ester or amide bonds; such a release may have species differences. For example, mice and humans are much different in

terms of carboxylesterase activity [55]. Drug release data for mice may thus need reevaluation for humans. All these issues are important for understanding and utilizing the PK/PD of drug–polymer conjugates, drug-encapsulated macromolecular drugs, and nanomedicines.

3. Unique features of blood vessels in tumors: angiogenesis, hypervascularity, irregularity of blood flow, extensive vascular permeability, and abnormal lymphatic drainage

3.1. Abnormality of tumor blood vasculature: morphology

In contrast to normal tissues and organs, most solid tumors show a higher vascular density (hypervasculature), especially when tumors are small, some exceptions being pancreatic and prostate cancers and large metastatic liver cancers. This finding may relate to the heterogeneity of the EPR effect, as discussed above. Tumor angiogenesis is now well known to be one of the most important features that sustains rapid tumor growth. Folkman [56–58] first demonstrated that tumors generate an angiogenesis-stimulating factor (now called vascular endothelial growth factor, or VEGF). Tumor angiogenesis was said to begin as the tumor diameter becomes larger than 0.8–1.0 mm [56–58], and the neovasculature being formed maintains the tumor blood supply. Our scanning electron microscopy (SEM) observations showed the presence of tumor vascular angiogenesis (vascular bed) even when tumor nodules were smaller than 0.2 mm [12,59].

The newly formed tumor blood vessels usually had an abnormal architecture, including defective endothelial cells with wide fenestrations, irregular vascular alignment, lack of a smooth muscle layer or innervation, wide lumen and impaired functional receptors for angiotensin II (AT-II) [10,12,29,59–65]. Blood flow behavior, such as direction of blood flow, was also irregular or inconsistent in these vessels [61]. Suzuki et al. [62] described unresponsiveness of tumor blood vessels to AT-II, and Hori et al. [61,66] observed tumor blood flow only once in 15–20 min, after which it stopped for a while; in addition, blood frequently flowed in the opposite direction.

3.2. Lymphatic clearance of tumor tissue and lymphatic metastasis

Tumor tissues usually lack effective lymphatic drainage [7,9,28–30,67]. In normal tissues, the lymphatic system can effectively recover macromolecules and lipid particles from the interstitial space. For instance, Lipiodol (iodinated poppyseed oil) is used for lymphangiography, because it is primarily recovered via the lymphatic system, and its presence in lymphatic vessels can be visualized with an X-ray system. The same recovery route was observed for macromolecular drugs. Maeda's group was the first to use Lipiodol as a carrier of the drug SMANCS. They found that when SMANCS solubilized in Lipiodol was injected into a tumor-feeding artery (e.g., via the hepatic artery for hepatomas and the renal artery for renal cell carcinomas), it selectively remained in tumor tissues, not in normal tissues [18,30,67,68]. Similarly, when the Evans blue/albumin complex was injected i.v. into tumor-bearing mice it accumulated and remained in the tumor for more than a week, but it was gradually cleared from nontumor tissue by normal lymphatic function [7]. As shown in Fig. 2A, Evans blue/albumin extravasated out of tumor tissue (i.e., into normal skin seen outside of the encircled tumor tissue), was gradually carried away via the lymphatic system, and disappeared in 1–2 weeks. No such clearance of Evans blue/albumin was found for tumor tissues.

In addition, although the lymphatic system does not function properly in tumor tissues, it is the major route for metastasis of tumor cells into normal tissues. Lymphatic metastasis is one of the most formidable consequences of cancer progression, and its control is critically important [20,28,69,70]. SMANCS, as originally developed [20], exhibited lymphotropic accumulation similar to that noted for NCS [69]. We also reported significant antimetastatic activity of SMANCS in rat and rabbit tumor models [20,28,70,71]. In addition, in metastatic liver cancer originating from colon and gastric cancer in humans, arterial administration of SMANCS with Lipiodol resulted in accumulation of the drug in metastatic lymph nodes, with a marked therapeutic effect [72]. This accumulation of SMANCS in lymph node metastases did not occur via the lymphatic route but by the arterial blood supply, which thus demonstrated the EPR effect [72]. Macromolecular drugs should thus be effective for diagnosis and treatment of lymphatic metastasis.

These architectural and anatomical features of a tumor's vascular system constitute the foundation of the EPR effect, which leads to extravasation of macromolecular and lipid drugs. In our recent collaboration with Professor Christophi's group at the University of Melbourne, we used a metastatic liver tumor model in mice to validate the anatomical characteristics of tumor blood vessels. In contrast to blood vessels in normal tissues, which possessed a uniform network and orientation (Fig. 4A–C), tumor blood vessels clearly showed abnormal vascular networks and exhibited high permeability, as evidenced by leakage of acrylic polymer resin as seen with SEM (Fig. 4D,E, indicated by arrows in E). Moreover, EPR effect-based treatment of tumor micronodules by use of the micellar form of pirarubicin completely destroyed the vascular bed of the tumor micronodules, so that the micronodules were no longer visible (Fig. 4F).

4. Factors involved in the EPR effect

Vascular mediators involved in the EPR effect include the following: (a) bradykinin (kinin), which is produced via activation of the kallikrein–kinin system involving a proteolytic cascade [9,28,73–76]; (b) NO generated from L-arginine by the inducible form of NO synthase (iNOS) in leukocytes and tumor cells [76–78], as well as peroxynitrite ($ONOO^-$), an oxidative derivative of NO [79]; (c) prostaglandins (PGs) [76,80]; (d) angiogensin-converting enzyme (ACE) inhibitors [66] and (e) vascular permeability factor (VPF)/VEGF and other cytokines [81–85].

Reducing pericyte coverage of tumor blood vessels by using transforming growth factor-β inhibitor was recently reported to greatly increase the intratumor uptake of nanoparticles [86], which suggested that this inhibitor, in combination with macromolecular anticancer drugs, has the potential to obtain better accumulation of drugs in tumors and thus an improved therapeutic effect. All the factors mentioned above are known as inflammatory mediators. That is, tumor tissues are like inflammatory tissues and show increased extravasation of macromolecules in plasma. The EPR effect can also be observed in inflammatory tissues. As described above, normal tissues surrounding tumors were affected by these vascular mediators and, similar to inflammatory tissues, showed extravasation of Evans blue (Fig. 2A).

4.1. Bradykinin (kinin)

Kinin is a major mediator of inflammation that induces extravasation and accumulation of body fluids in inflammatory tissues (edema); it is the major cause of pain in inflammation [87,88]. Maeda et al. [73] found that tumors have, in addition to bradykinin (also referred to as kinin), [hydroxyprolyl^3]bradykinin, which is a derivative of kinin that has the third amino acid replaced by hydroxyproline. High levels of the derivative were found in blood plasma and in peritoneal and pleural fluids in carcinomatosis in patients with advanced cancer [73–75]. This increased kinin is generated by tumor cells through activation of the Hageman factor (factor XII) and then the pathway of prekallikrein to kallikrein to kinin [74,76]. Administration of kinin at the nanomolar level into the skin of guinea pigs significantly increased the permeability of blood vessels and thus the accumulation of Evans blue at the injection site [60]. Inhibition of kinin generation by means of kallikrein inhibitors (e.g., soybean

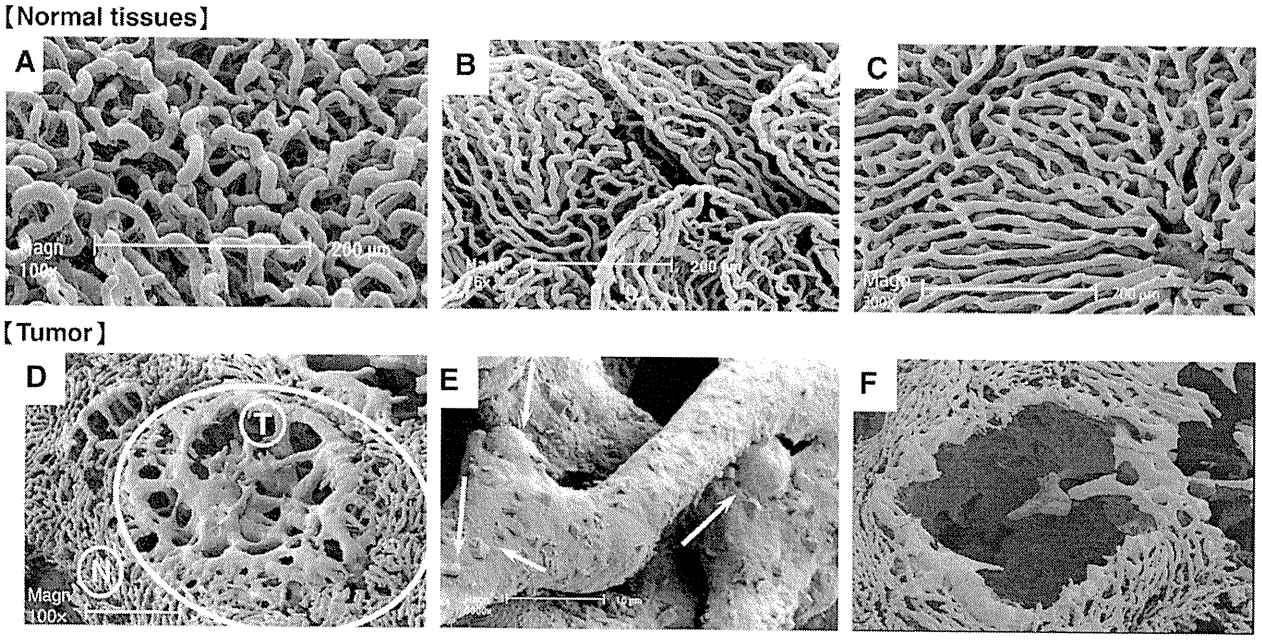

Fig. 4. SEM images of blood vessels in various normal tissues (A–C) and metastatic liver tumors (D–F). Normal capillaries of the pancreas (A), colon (intestinal villi) (B), and liver (sinusoid) (C) are shown. (D) Metastatic tumor nodule (circled area identified with T) in the liver, the normal liver tissue is indicated with "N." (E) Tumor vessels at the capillary level (larger magnification), with a rough surface and an early phase of polymer-extravasating vessels (arrows). Normal tissues show no leakage of polymeric resin (A–C), whereas the tumor nodules clearly demonstrate tumor-selective extravasation of polymer (via the EPR effect) (D, E). After i.v. injection of the macromolecular anticancer drug (SMA-pirarubicin micelles), the tumor vascular bed (visible in D) was completely disintegrated, as shown by an empty void (F).
Modified from Ref. [11] with kind permission of J. Daruwalla and C. Christophi.

trypsin inhibitors, SBTIs) or the kinin antagonist HOE-140, however, significantly suppressed fluid accumulation in mice bearing ascites tumor [73–76].

Moreover, we and other research groups previously reported that the kinin type 2 (B2) receptor was highly expressed in human and animal tumor tissues [89–91]. Kinin is also known to activate endothelial cell-derived NO synthase [92], which ultimately leads to an increase in NO, which is an important mediator of tumor vascular permeability, as described below. Therefore, vascular permeability in tumors is commonly associated with kinin, both directly and indirectly.

4.2. NO and its derivatives, and collagenase (matrix metalloproteinase)

NO is a vital molecule in living creatures, since it has multiple direct and indirect roles as a signaling messenger. NO is produced from L-arginine by NOS in the presence of oxygen. In inflammation and cancer, NO is extensively produced from a greatly increased number of infiltrated leukocytes, in which iNOS plays a major role. To study the role of NO in cancer, we prepared an oily formulation of NO (a solution of NO in medium-chain triglycerides). Intradermal injection of this formulation into guinea pigs caused marked extravasation of Evans blue-/albumin complex at the injection site [78]. The extravasation was significantly inhibited by the NO scavenger carboxy-2-phenyl-4,4,5,5-tetramethylimidazoline-1-oxyl-oxide (cPTIO) [77]. In *in vivo* experiments with a tumor-bearing mouse model, we showed that both cPTIO and the NOS inhibitor N^{ω}-monomethyl-L-arginine (L-NMMA) inhibited extravasation of Evans blue in tumors [76]. Tumors also showed extensive iNOS expression, which indicated that tumors produce significantly more NO compared with normal tissues [77,93] (Fig. 5A). The amount of NO produced in tumors has a positive association with tumor weight—up to 1.75 g in AH136B tumor-bearing rats and 250 mg in mice bearing sarcoma 180 (S-180) tumors; this result corresponds to the extravasation of the Evans blue/albumin complex (the EPR effect) [77,78] (Fig. 5B,C). iNOS knockout mice evidenced clearly delayed tumor growth after tumor cells were injected into the mice [94]. Thus, NO generation is important for tumor growth, and to maintain the supply of nutrients and oxygen.

Like NO, oxidized products of NO including $ONOO^-$ and nitrogen dioxide potentiated the EPR effect. Among the NO derivatives, $ONOO^-$ is a strong oxidizing and nitrating agent, which forms via the reaction of NO with superoxide anion ($O_2^{\bullet-}$) at a diffusion-limited rate [95,96]. Also like NO, $O_2^{\bullet-}$ is generated extensively in tumor and inflammatory tissues, primarily via NADPH oxidase and cytochrome b_5 reductase in infiltrated macrophages and neutrophils, plus XO [97–100]. In addition, Maeda's group showed that NOS can catalyze the generation $O_2^{\bullet-}$. The reductase domain of iNOS uses oxygen and nitroguanosine (a nitrosated product of guanosine by $ONOO^-$) as substrates to yield $O_2^{\bullet-}$ [101].

Intradermal injection of $ONOO^-$ increased extravasation of Evans blue/albumin in a dose-dependent manner at the site of injection (Fig. 6A). This extravasation lasted for a relatively long time after $ONOO^-$ administration (Fig. 6B) [79], even though the half-life of $ONOO^-$ at physiological pH is only a few seconds [102]. This finding suggests a secondary or indirect mechanism in $ONOO^-$-induced enhancement of the EPR effect. One major mechanism that we demonstrated involves activation of matrix metalloproteinases (MMPs) [79]. MMPs are classified as zinc-dependent neutral endopeptidases that are expressed at high levels in tumor cells and play important roles in tumor invasion, metastasis, and angiogenesis [103–107]. Activation of MMPs causes disintegration and remodeling of the extracellular matrix, in addition to facilitating vascular permeability via degradation of matrix proteins as a result of collagenolytic action; MMPs probably affect blood vessels as well. $ONOO^-$ can be decomposed to generate NO, which leads to functioning of the EPR effect. It may also enhance the EPR effect through a kinin cascade via activation of MMPs as follows: $ONOO^- \rightarrow$ proMMP $\rightarrow$ MMP $\rightarrow$ plasminogen/miniplasminogen $\rightarrow$ prekallikrein $\rightarrow$ kallikrein $\rightarrow$ kinin [79].

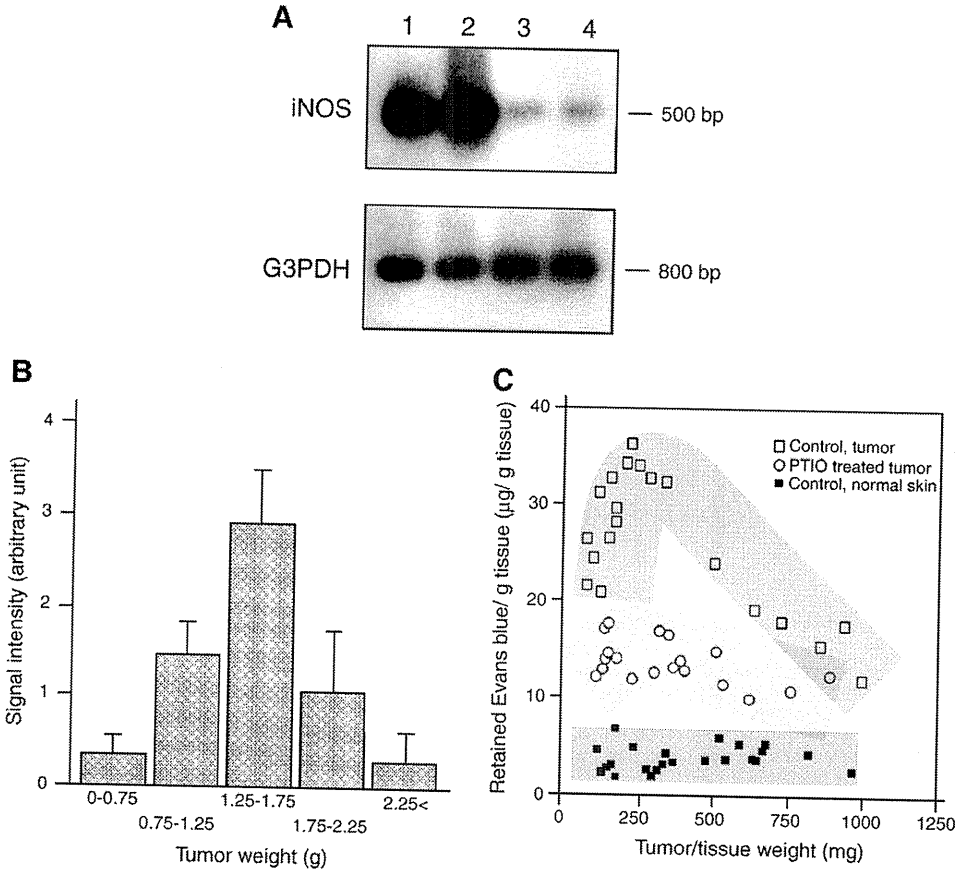

Fig. 5. NO production in different tumors. (A) RT-PCR for iNOS mRNA expression in rat AH136B solid tumor is shown: lanes 1 and 2 are results for AH136B tumor obtained from two different rats, and lanes 3 and 4 are results for two normal livers. (B) Correlation of the concentration of NO, as determined by the signals of NO-*N*-dithiocarboxysarcosine (DTCS)-Fe^{2+} being formed in solid tumor (AH136B) with tumor weight. Rats received i.v. injections of DTCS-Fe^{2+} complex, followed by electron paramagnetic resonance measurement at 110 K. Data are expressed as means ± SE. (C) Association between S-180 tumor weight in mice and the extent of extravasation of Evans blue/albumin in tumor (the EPR effect), and the concentration of NO in tumors of different size. PTIO is an NO scavenger [130]. Tumors weighing up to 1.75 g in rats (B) and 250 mg in mice (C) showed size-dependent NO production and extravasation of Evans blue/albumin.
Modified from Refs. [77] and [78].

In addition, the high reactivity of $ONOO^-$ leads to rapid production of nitrate or nitrosated aromatic residues including proteins and nucleic acids, and thus generation of nitrotyrosine and nitroguanosine [79,97–99,101,108]. These nitro compounds are likely to release nitrite (NO_2^-) and may serve as a source of NO. As discussed later, nitroglycerin (NG) would be converted to NO to facilitate the EPR

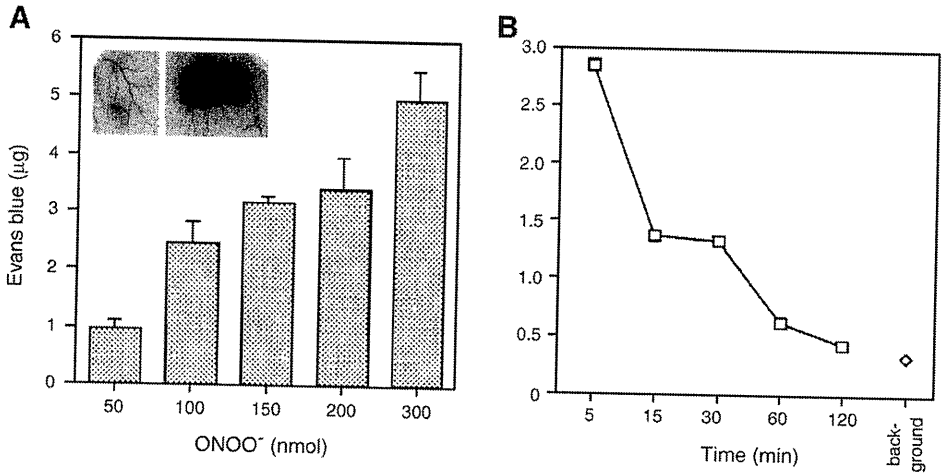

Fig. 6. Dose-dependent effect of $ONOO^-$ on vascular permeability of dorsal skin in normal mice (A) and duration of the enhancement of vascular permeability (B). (A) $ONOO^-$ was injected intradermally at the indicated concentrations. The inset shows authentic $ONOO^-$-induced vascular permeability in mouse skin (left: decomposed $ONOO^-$, right: $ONOO^-$ 100 nmol). (B) Evans blue (10 mg/kg) was given by i.v. injection at 10, 15, 30, 60, or 120 min after intradermal injection of 100 nmol $ONOO^-$ into dorsal skin; dye extravasated for 1 h.
From Ref. [79] with permission.

effect. Multiple mechanisms of enhancement of vascular permeability by $ONOO^-$ therefore exist and are a consequence of cross-talk in the vascular mediator network.

4.3. Prostaglandins

PGs are lipid compounds that are derived enzymatically from arachidonic acid by means of cyclooxygenases (COXs) [76,80]. Similar to bradykinin, PGs are important mediators in inflammation and can be upregulated by inflammatory cytokines (e.g., interleukin-1 and tumor necrosis factor-α) as well as kinin [109,110]. Among the various PGs, PGE_1 and PGI_2 exhibit effects similar to those of NO, i.e., preventing platelet aggregation, leukocyte adhesion, and thrombosis formation and facilitating extravasation and the EPR effect. As we anticipated, we found significantly decreased accumulation of the Evans blue/albumin complex in tumors after administration of a COX inhibitor to tumor-bearing mice [76]. Injection of a stable analogue of PGI_2, beraprost sodium (Dorner), which has a long plasma half-life in humans (1.1 h compared with several seconds for native PGI_2), resulted in significantly increased extravasation. Beraprost enhanced the accumulation of the Evans blue/albumin complex 2- to 3-fold [111]. An important and interesting finding was that systemic blood pressure did not change significantly, nor was blood flow of normal tissues and organs affected, whereas blood flow in tumors was dramatically suppressed (70–90%). Beraprost not only enhanced the EPR effect but also inhibited tumor growth [111]. The therapeutic potential and the possible diagnostic applications of beraprost thus warrant more detailed studies.

4.4. Angiotensin-converting enzyme (ACE) inhibitors

ACE inhibitors are a landmark class of drugs for hypertensive patients. They inhibit conversion of angiotensin I to AT-II by carboxypeptidase. The amino acid sequence of angiotensin I (Asp-Arg-Val-Tyr-Ile-His-Pro-Phe-His-Leu) is similar to that of bradykinin (Arg-Pro-Pro-Gly-Phe-Ser-Pro-Phe-Arg) at the C-terminal end, so inhibition of ACE blocks degradation of bradykinin as well. ACE inhibitors therefore potentiate the pharmacological actions of kinin, which is a major vascular permeability factor as discussed above, the result being augmented extravasation of the Evans blue/albumin

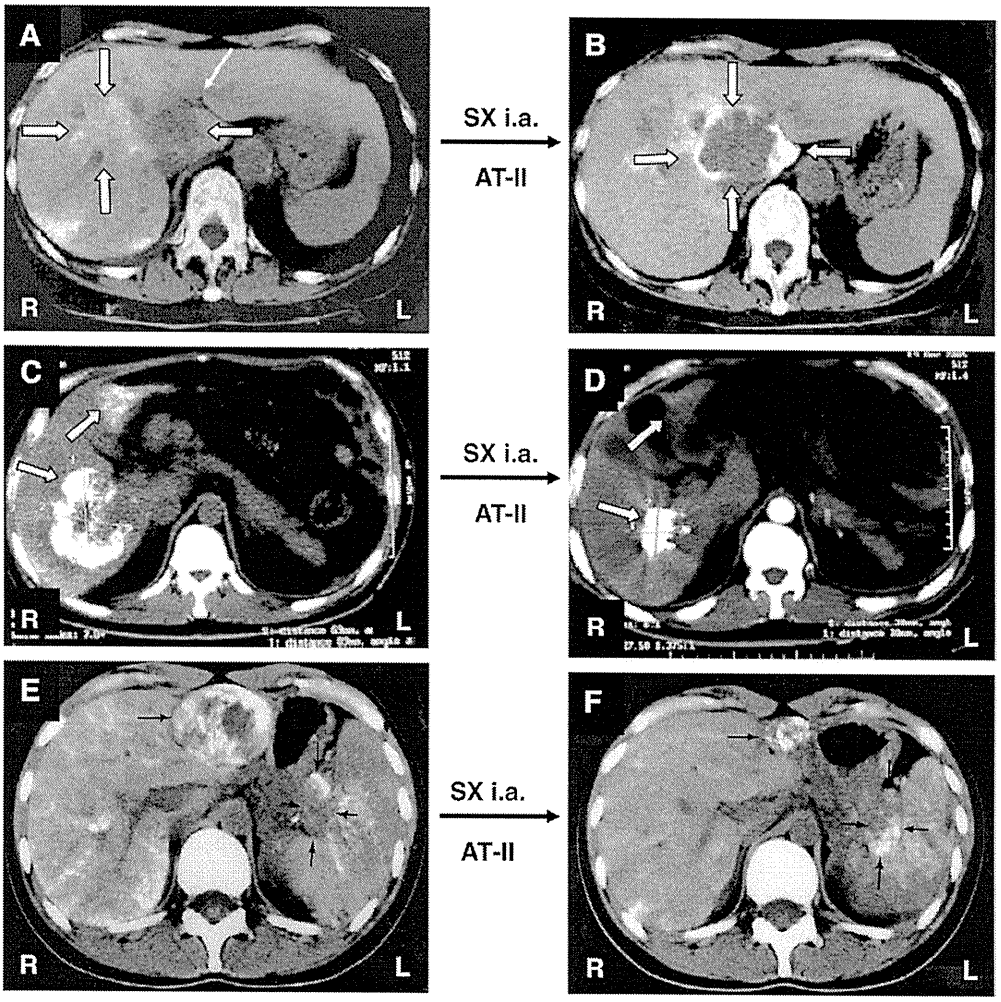

Fig. 7. Responses of human metastatic liver cancers to SMANCS/Lipiodol (SX/LP) under AT-II-induced hypertension. (A and B) CT scans of a patient with metastatic liver cancer after an i.a. injection of SX/LP under normotensive (A) and hypertensive (B) conditions. A clear difference can be seen from normotensive to hypertensive conditions in tumor uptake of SX/LP, as indicated by arrows pointing to high-density areas. B-type staining (i.e., a peripheral ring shape), which is usually seen in metastatic tumors on CT scans (B), indicates greater drug uptake under AT-II-induced hypertension. A massive metastatic liver cancer that originated from stomach cancer is shown in (C). At 50 days after SX/LP treatment, this liver cancer had regressed considerably (D). (E and F) A massive metastatic liver cancer originating from pancreatic cancer. A CT scan shows the metastatic mass in the liver (center front) and the primary pancreatic cancer (left middle) at the time of the first SX/LP infusion (E). The large metastatic mass at center front did regress markedly at 5 months after four SX/LP injections given under AT-II-induced hypertension (F). The primary pancreatic cancer did also take up SX/LP (F). R and L indicate the right and left sides of the patient, respectively. Modified from Ref. [19] with permission.

complex into tumor tissues, an effect similar to that of beraprost [66,111].

4.5. Vascular endothelial growth factor

VEGF is the angiogenesis factor that is highly upregulated in most tumors, and it has a crucial function in angiogenesis and solid tumor growth [60,81,83,84,112]. Folkman [56–58] and Ferrara and Henzel [82] played a most important role in the discovery and clinical development of VEGF. However, Dvorak's group first reported VEGF as VPF in 1983 [81,113]. Since those discoveries, researchers have conceived of an inhibitor of VEGF as being a useful therapeutic tool against solid tumors. After decades of research, inhibitors of VEGF have been developed as therapeutics, e.g., bevacizumab (Avastin) and ranibizumab (Lucentis). Other researchers and we previously reported that the amount of VEGF was higher (2- to 30-fold) in many implanted murine tumors than in most normal tissues and organs [60]. The degree of potency of VEGF in inducing extravasation (the EPR effect) was comparable to that of kinin in guinea pig skin seen after intradermal injection [60]. Additional studies by different groups indicated that VEGF action involves upregulating NO production [114,115].

4.6. Summary of EPR-related factors

Thus, briefly, the EPR effect is a result of multifactorial events *in vivo*, and interaction among factors influencing it makes it quite complicated. Like many inflammatory cytokines, these vascular factors affect each other via cross-talk. Inhibition of one factor, for example by the MMP inhibitors SI-27 (L-*N*-(*N*-hydroxy-2-isobutylsuccinamoyl)-leucyl-isobutylamide) and BE16627B (L-*N*-(*N*-hydroxy-2-isobutylsuccinamoyl)-seryl-L-valine), may block the EPR effect to a significant extent but not completely [79]. Activation of one factor, however, would lead to induction of multiple steps of the cascade, thereby involving activation of many factors. A greater than 1:1 correlation between the initial activation and the end result would occur, so that a significant EPR effect would rapidly ensue. Studies of these factors may therefore help development of new strategies to modulate the EPR effect, angiogenesis and thereby tumor growth.

5. Augmentation of the EPR effect

Many macromolecular anticancer drugs are being developed on the basis of the EPR effect. To improve the therapeutic efficacy of these drugs, we focused on the unique pathophysiological features associated with the EPR effect, as described above. We first used AT-II, which produces systemic hypertension. Under these hypertensive conditions, a macromolecular drug is pushed out by hydrodynamic forces into the interstitial space or matrix of tumor tissues. A second method utilizes NO-releasing compounds to enhance the EPR effect. Both methods exhibited favorable therapeutic effects in clinical settings, as described here.

5.1. Increased delivery of macromolecular drugs to tumors under AT-II-induced hypertension

Tumor blood vessels usually lack a smooth muscle layer or pericytes needed for vasoconstriction, so tumor blood vessels show very little response to infusion of AT-II, whereas blood vessels of normal tissues show constriction (hence hypertension). One would expect, therefore, that during induction of the hypertensive state by AT-II, normal blood vessels would constrict but tumor blood vessels would be open, which would facilitate the vascular leakage. The outcome would be increased blood flow volume in tumor tissues and hence increased drug delivery.

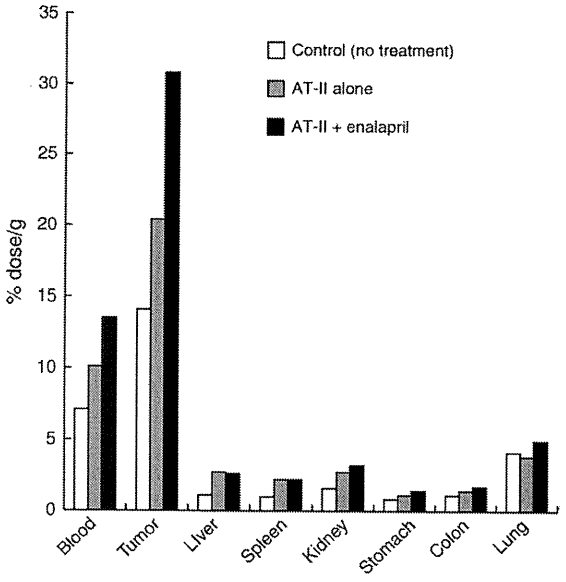

Fig. 8. Effects of AT-II alone or AT-II plus enalapril on accumulation of macromolecular drugs. Tissue distribution of ^{125}I-labeled A7 antibody 3 days after i.v. injection. Nude mice ($n=4$) bearing SW1116 human colon carcinoma cells were treated with AT-II alone or AT-II plus enalapril. From Ref. [131] with permission.

In such situations, macromolecules such as albumin, SMANCS, micelles, liposomes and lipid particles (e.g., Lipiodol) leak out more from tumor vessels, the result being augmentation of the EPR effect [19,29]. Under AT-II-induced hypertension, blood flow volume in normal tissues, in contrast to that in tumor vessels, remains constant by means of an autoregulatory mechanism, even though the blood vessels are constricted. This important tumor-selective phenomenon was first reported by Suzuki et al. [62] in 1981. They first applied this method of hypertensive chemotherapy with conventional, low-molecular-weight anticancer agents, but with little success. Even though AT-II-induced hypertension should increase drug delivery, the tumor accumulation was maintained for no more than 15 min for low-molecular-weight agents, as we found for [^{14}C]methylglucose delivered to tumors in a rat model [116]. The therapeutic benefit is thus quite limited for low-molecular-weight anticancer drugs. In contrast, when we utilized AT-II-induced hypertension with macromolecular drugs, we observed an approximate 2-fold increase in the EPR effect, as well as less adverse effect to normal tissues including bone marrow, liver, kidney and colon [19,29,116]. Not only has augmentation of the EPR effect by means of AT-II proved effective in preclinical (animal) experiments, but it has also been validated in clinical settings with difficult-to-treat tumors, even those of an advanced stage [19]. AT-II was utilized during an i.a. infusion of SMANCS for patients with such advanced cancers. For these cases, SMANCS was formulated with the lipid contrast agent Lipiodol (SMANCS/Lipiodol), which has been commonly used in Japan to

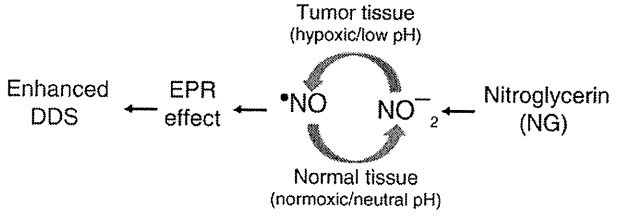

Fig. 9. Mechanism of NO generation from nitroglycerin in tumor. NO was generated from NO_2^- predominantly in hypoxic tumor tissues compared with normal tissues. DDS, drug delivery system.
From Ref. [121] with permission.

treat hepatocellular carcinoma (HCC) since 1993, although under normotensive conditions.

To augment drug delivery, AT-II was first given by slow i.v. infusion to induce a hypertensive state (i.e., to increase mean arterial blood pressure by 20–25%, for example, from a systolic blood pressure of 110 mm Hg to 150 mm Hg). The drug was then administered by i.a. infusion (via Seldinger's method). With this method, we obtained a marked therapeutic effect, not only for HCC but also for metastatic liver cancers [19]. A few typical examples are described here. As Fig. 7A shows, with SMANCS/Lipiodol infusion first performed under normotensive conditions for colon cancer metastatic to the liver, only a very limited area of the tumor mass evidenced staining, and most of the other area (especially the central part of the tumor) was dark (i.e., was of low density on the CT scan), which suggests no uptake of SMANCS/Lipiodol under normotension. However, 1 week later, after SMANCS/Lipiodol was administered under AT-II-induced hypertension, marked staining with SMANCS/Lipiodol was evident, especially at the tumor periphery (Fig. 7B). This typical pattern of staining of metastatic tumors is classified as B-type staining [18]. This result demonstrates the central hypovascularity of the tumor. After 3 months, another infusion of SMANCS/Lipiodol was performed under AT-II-induced hypertension, which produced a marked accumulation of the drug, a reduction in levels of tumor markers (carcinoembryonic antigen and immunosuppressive acidic protein), and an improved performance status of the patient; in about 8 months, the tumor volume was one-fifth of the original [19]. The second example shown here confirmed a marked therapeutic effect of similar treatment (under hypertension) used for a patient with massive metastatic liver cancer originating from stomach cancer (Fig. 7C,D). Still another patient with metastatic liver cancer originating from pancreatic cancer (Fig. 7E,F) also evidenced marked regression of the tumor mass (to about 15% of the original) after four SMANCS/Lipiodol injections in 5 months. In this last patient (Fig. 7E,F), the original pancreatic cancer also accumulated SMANCS/Lipiodol. AT-II-induced hypertensive conditions produced complete filling of SMANCS/Lipiodol even in a hypovascular pancreatic tumor (Fig. 7F). These and many other examples confirmed that i.a. SMANCS/Lipiodol administered under AT-II-induced hypertension could augment the EPR effect and drug delivery and thereby induce a remarkable therapeutic effect. Similar results were observed with gallbladder, kidney and other intractable cancers. AT-II-induced hypertension can therefore be a powerful tool for augmenting the EPR effect, and we anticipate great improvements in results with macromolecular anticancer therapeutics under AT-II-induced hypertension.

In our previous unpublished studies, when AT-II was combined with the ACE inhibitor enalapril, which blocks kinin degradation, the accumulation of macromolecular drugs in tumors was significantly increased, which indicated a synergistic and/or additive effect (Fig. 8); enalapril had no influence on blood flow in normal tissues. The clinical importance of AT-II-induced hypertensive chemotherapy may thus be

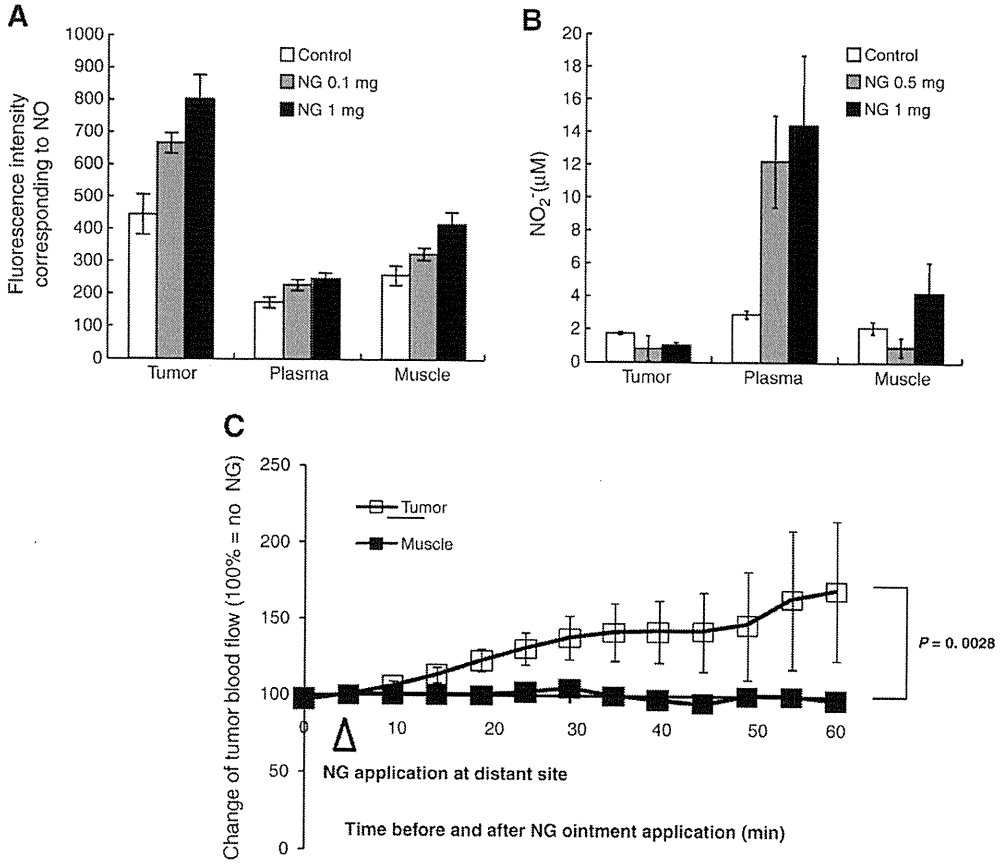

Fig. 10. NG-induced intratumor production of NO (A) and NO_2^- (B) and increased tumor blood flow (C). NG ointment was applied to S-180 tumor-bearing mice on the skin distal to the tumor at the indicated concentrations. After specified intervals, mice were killed and tumors were collected and homogenized. NO was detected in the supernatant of tumor tissue homogenate by using the fluorescent probe DAF (A) or by measuring NO_2^- with HPLC (B). (C) Blood flow in normal tissues and in tumors with diameters of 6–7 mm was measured with a laser Doppler flowmeter, after mice had been anesthetized and placed on a warm pad (30–35 °C). Blood flow was monitored for the first 5 min to confirm that it was stable, and then NG at dose of 1.0 mg/tumor was applied on the tumor. Blood flow in the thigh muscle was measured after application of the same dose of NG on the skin. Modified from Ref. [121] with permission.

further improved by including an ACE inhibitor, which is known to be a very safe, routinely used drug. Additional investigations of this method are warranted.

5.2. Enhanced delivery of drugs to tumors by means of NG

Because NO is a major factor that facilitates the EPR effect, we expected that the EPR effect or tumor-targeted delivery of macromolecular anticancer drugs might be enhanced by use of NO or NO-releasing compounds.

With reference to a separate but related topic, even though Jordan et al. [117] did not discuss drug delivery or the EPR effect, they reported that isosorbide dinitrate (ISDN) increased the partial oxygen pressure (pO_2) in tumor tissues as related to increased blood flow, and Mitchell et al. [118] showed that NO_2^- increased tumor cell radiosensitivity because of increased tissue pO_2.

In our laboratory, we investigated NG and ISDN to determine whether they would enhance the EPR effect. NG is a well-known NO-generating agent and has been used as medication for angina pectoris for more than a century. In cardiac infarct tissue, NO_2^- is first liberated from NG and is then converted to NO under hypoxic conditions (Fig. 9) [119,120]. Vasodilatation and increased blood flow can thereby be attained in infarcted tissues. The pO_2 in cardiac infarct tissue is known to be low, and the pH is slightly acidic [117,118]. These conditions are similar to those in cancer tissues, which are hypoxic and slight acidic. We thus hypothesized that NG may induce the same processes in tumor tissues as in cardiac infarct tissues (Fig. 9). If the same mechanism does operate in solid tumors, macromolecular drug delivery (the EPR effect) and hence therapeutic efficacy of these drugs may be enhanced by applying NG.

As we hypothesized, we obtained astonishing results in various rodent tumor models [121]. We first quantified the amount of NO in tumor and normal tissues after NG treatment, by using an NO-specific fluorescent agent, diaminofluorescein (DAF) [122]. Administration of NG induced a significant (e.g., 2 folds) increase in NO dose-dependently in tumor tissue, whereas normal tissues showed no significant increase (Fig. 10A). Similarly, NO_2^- production in tumor tissue after NG administration increased in a dose-dependent manner, as quantified by using Griess reagent (Fig. 10B), and the high level of NO_2^- lasted at least for 3 h (data not shown). Consistent with the increased NO level, blood flow in tumor tissue was significantly elevated (Fig. 10C) [121]. This finding is similar to that for ISDN in the report mentioned previously [117]. These results in tumor-bearing animals are therefore analogous to the effects of NG seen in cardiac patients.

Subsequently, when tumor-bearing mice received topical applications of NG ointment, over the tumor or on skin opposite or distal to the tumor site, at doses of 1.0 μg/mouse to 1.0 mg/mouse, the EPR effect was greatly increased in a dose-dependent manner. Namely, NG treatment significantly augmented accumulation of both the Evans blue/albumin complex and the macromolecular anticancer drug PEG-conjugated zinc protoporphyrin (PZP) in all tumors including S-180, Meth-A and colon-38 in mice, and breast cancer in rats induced by 7,12-dimethylbenz[*a*]anthracene (DMBA) [121]. The NG-enhanced EPR effect lasted more than 24 h after a single application [121], which was consistent with the sustained efficacy of NG given to patients for angina pectoris. Consequently, the therapeutic effect of PZP was markedly enhanced when PZP was combined with NG in all the mouse tumor models (Fig. 11) [121]. The NG/NO-enhanced drug delivery to tumor and hence improved antitumor effect were found as well with the anthracycline antitumor agent aclarubicin (Fig. 11B), which is a conventional low-molecular-weight drug [121]. It is

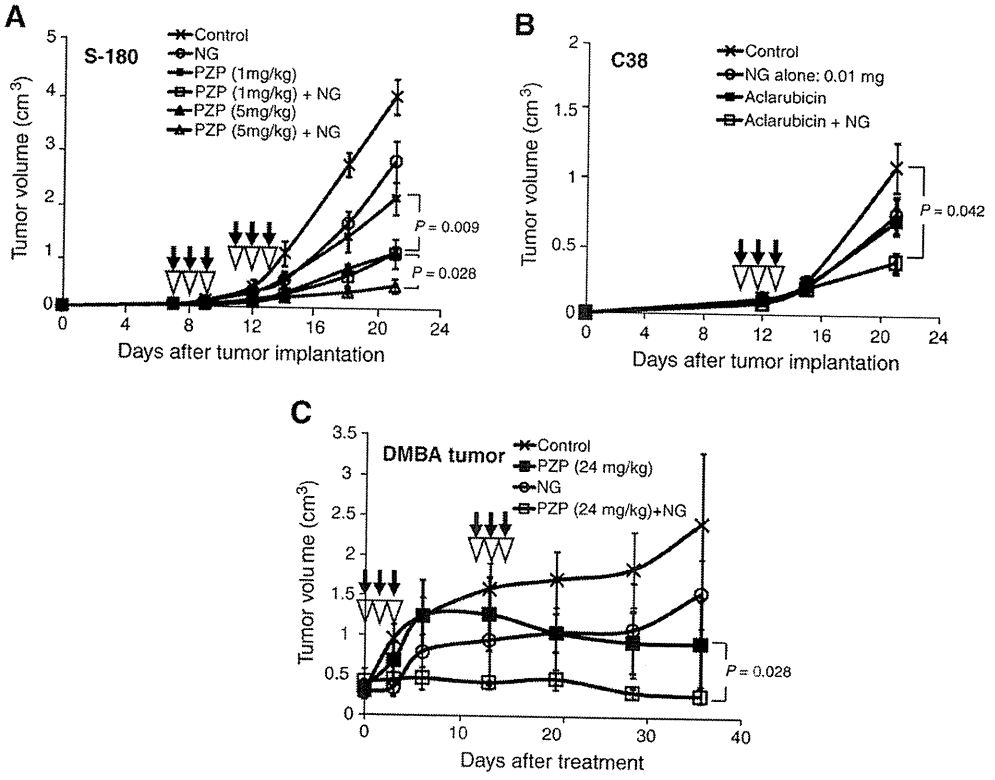

Fig. 11. Enhancement of the therapeutic effect of antitumor drugs by NG treatment. (A) The effect of the combination of NG (0.1 mg/tumor) and the macromolecular drug PZP against S-180 solid tumors. (B) The effect of NG (0.01 mg/tumor), alone and in combination with the low-molecular-weight drug aclarubicin (5 mg/kg), against colon-38 solid tumors. (C) Therapeutic effect of PZP plus NG (0.1 mg/tumor) in DMBA-induced breast tumors in rats. Black arrowheads indicate the times of drug administration; open inverted triangles indicate the times of NG treatment.
Modified from Ref. [121] with permission.

intriguing that NG alone also had significant suppressive effects on tumor growth (Fig. 11B) [121]. All these findings therefore suggest that use of NG may become a promising strategy for cancer treatment in patients, to enhance the effect of not only macromolecular anticancer drugs but also conventional chemotherapeutics.

The combination therapy of NO with anticancer drug was also reported by Passut et al. by using a polymer–drug conjugates carrying epirubicin (EPI) and NO (EPI-PEG-NO) that co-release the anticancer drug EPI and NO [123,124]. Even though no enhancement of EPR effect was discussed, they showed that NO released from EPI-PEG-NO inhibited cellular respiration followed by mitochondrial membrane depolarization and cell death in cancer cells but not in normal cells, which significantly increased the cytotoxic (antitumor) effect of EPI whereas remarkably reduced the cardiac toxicity of EPI [123–125]. Moreover, in clinical settings, Yasuda et al. [126–128] and Siemens et al. [129] independently reported direct therapeutic benefits of NO donors. They indicated that the possible anticancer mechanism of NO is probably due to down-regulation of hypoxia-inducible factor-α, VEGF and P-glycoprotein. Yasuda et al. [126,127] demonstrated clinical benefits of NG in a randomized phase II study with patients with non-small cell lung cancer, in which NG significantly increased chemosensitivity to conventional anticancer drugs such as docetaxel, carboplatin, vinorelbine and cisplatin. Siemens et al. [129] analyzed the effect of an NO donor on prostate cancer patients after primary therapy (either surgery or radiotherapy) and showed that the doubling time of the prostate-specific antigen value was significantly extended with NG treatment. These reports suggest not only that NG/NO may show synergistic and/or additive effects with other anticancer drugs, probably by augmenting tumor drug delivery, but also that NO itself appears to have a tumor-suppressive effect.

These findings together indicate that AT-II-induced hypertension and NG-derived NO can augment the EPR effect and hence the chemotherapeutic effect of macromolecular drugs. Further investigations of this new anticancer strategy are consequently warranted.

6. Other issues related to the EPR effect

The discussion just presented indicates that the EPR effect is clearly understood to improve targeting of drugs to tumors. However, the EPR effect has other consequences: for example, it facilitates the transport to tumors of nutrients and oxygen that sustain rapid tumor growth. Tumor growth can thus be suppressed by inhibiting or blocking the EPR effect in tumor tissues, i.e., by reducing angiogenesis and extravasation. Certain drugs in clinical use may suppress the EPR effect, for example, VEGF inhibitors such as bevacizumab and ranibizumab, as described above.

Also, with regard to the kallikrein–kinin cascade, Maeda's group reported suppression of ascitic and solid tumors by use of a kallikrein inhibitor (SBTI, Kunitz type) and the kinin antagonist HOE-140 [73–76]. In a mouse S-180 ascitic tumor model, intraperitoneal (i.p.) administration of SBTI significantly reduced the ascitic volume (Fig. 12A) [74]. Similarly, HOE-140 treatment (i.p. injection) significantly inhibited accumulation of ascites in tumor-bearing mice (Fig. 12B), as well as significantly increasing the survival of these mice (Fig. 12C). Furthermore, a therapeutic effect was found for HOE-140 in S-180 solid tumor model: HOE-140 treatment caused an approximate 50% reduction in tumor volume (Fig. 12D) [76]. These findings suggest that inhibition of

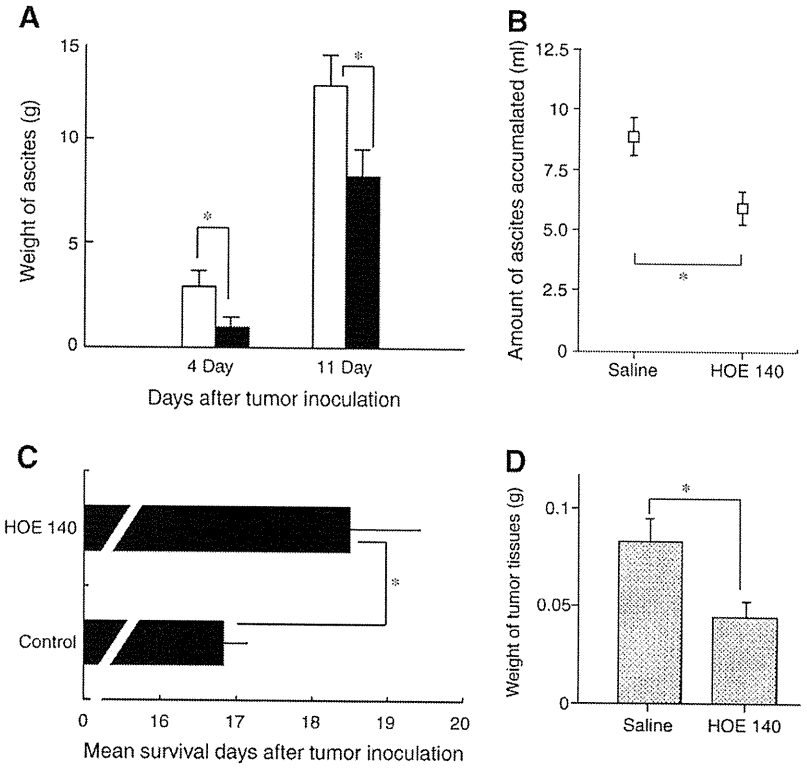

Fig. 12. Effects of SBTI and HOE-140 on tumor growth and survival of mice. (A) SBTI (3 mg/mouse per day i.p.) was administered for 10 days beginning from the day of S-180 ascitic tumor injection. White and black columns indicate the control group and the SBTI-treated group, respectively. (B) HOE-140 was given at a dose of 13 μg/kg i.p. starting immediately after tumor injection, with ascitic fluid collected 10 days after tumor injection. The effects of this HOE-140 treatment on survival of ascitic tumor-bearing mice (C) and S-180 solid tumor growth in mice (D) are shown. *$P<0.05$.
Modified from Refs. [74] and [76] with permission.

the EPR effect, by using agents such as HOE-140 and SBTI, may produce an antitumor effect via an alternative mechanism. In patients with carcinomatosis, ascitic or pleural effusion is one of the most dangerous conditions; however, it is often overlooked in drug development. The findings that we just discussed may suggest a clue for the solution to this problem.

7. Conclusions

Macromolecular anticancer drugs are receiving more attention than ever in cancer chemotherapy, because the most important mechanism for targeting of drugs to tumors—the EPR effect—would improve therapeutic efficacy and reduce adverse effects, compared with conventional chemotherapy with low-molecular-weight drugs. The EPR effect is the unique and most crucial phenomenon occurring in tumor tissues, in that it accounts for the anatomical and pathophysiological characteristics of tumor blood vessels. The EPR effect is mediated by various upregulated vascular factors such as kinin, NO, VEGF and PGs. A strategy to augment the EPR effect and hence anticancer drug effects by modulating these factors seems reasonable. Among methods to augment the EPR effect, AT-II-induced hypertension has been validated as effective in both experimental and clinical studies. Also, the NO-releasing compound NG is promising for enhancing both the EPR effect and consequent therapeutic effects of anticancer drugs, especially macromolecular drugs.

In summary, the EPR effect is the gold standard for macromolecular anticancer drug design. However, its limitations—such as the PEG dilemma and the heterogeneous consequences of the effect—must be addressed, perhaps by making use of different strategies such as SMA micelles. For example, we found better cellular uptake (about 5-fold better) for SMA micelles than for PEG micelles. We thus anticipate great progress in the development of macromolecular therapeutics because of the advantages of the EPR effect.

Acknowledgements

The work included in this paper was supported in part by the Cancer Priority Grant and other grants from the Ministry of Education, Culture, Sports, Science and Technology of Japan (no. 20590049, no. 20015045 and no. S0801085). We thank Ms. J. Daruwalla and Professor C. Christophi of the University of Melbourne, Australia, for their courtesy in allowing us to use Fig. 4, and Dr. Y. Ishima of the Graduate School of Pharmaceutical Sciences, Kumamoto University, Japan for his excellent technical assistance with Fig. 10B. The authors also acknowledge the literature survey for the citation of the EPR effect (Fig. 1) by Dr. Arun K. Iyer and Mr. Gahininath Y. Bharate of our Department at Sojo University.

References

[1] Editorial, Welcome clinical leadership at NICE, Lancet 372 (2008) 601.
[2] J. Tol, M. Koopman, A. Cats, C.J. Rodenburg, G.J.M. Creemers, J.G. Schrama, F.L.G. Erdkamp, A.H. Vos, C.J. van Groeningen, H.A.M. Sinnige, D.J. Richel, E.E. Voest, J.R. Dijkstra, M.E. Vink-Borger, N.F. Antonini, L. Mol, J.H.J.M. van Krieken, O. Dalesio, C.J.A. Punt, Chemotherapy, bevacizumab, and cetuximab in metastatic colorectal cancer, N. Engl. J. Med. 360 (2009) 563–572.
[3] T. Fojo, C. Grady, How much is life worth: cetuximab, non-small cell lung cancer, and the $440 billion question, J. Natl. Cancer Inst. 101 (2009) 1044–1048.
[4] L.D. Wood, D.W. Parsons, S. Jones, J. Lin, T. Sjöblom, R.J. Leary, D. Shen, S.M. Boca, T. Barber, J. Ptak, N. Silliman, S. Szabo, Z. Dezso, V. Ustyanksky, T. Nikolskaya, Y. Nikolsky, R. Karchin, P.A. Wilson, J.S. Kaminker, Z. Zhang, R. Croshaw, J. Willis, D. Dawson, M. Shipitsin, J.K. Willson, S. Sukumar, K. Polyak, B.H. Park, C.L. Pethiyagoda, P.V. Pant, D.G. Ballinger, A.B. Sparks, J. Hartigan, D.R. Smith, E. Suh, N. Papadopoulos, P. Buckhaults, S.D. Markowitz, G. Parmigiani, K.W. Kinzler, V.E. Velculescu, B. Vogelstein, The genomic landscapes of human breast and colorectal cancers, Science 318 (2007) 1108–1113.
[5] T. Sjöblom, S. Jones, L.D. Wood, D.W. Parsons, J. Lin, T.D. Barber, D. Mandelker, R.J. Leary, J. Ptak, N. Silliman, S. Szabo, P. Buckhaults, C. Farrell, P. Meeh, S.D. Markowitz, J. Willis, D. Dawson, J.K. Willson, A.F. Gazdar, J. Hartigan, L. Wu, C. Liu, G. Parmigiani, B.H. Park, K.E. Bachman, N. Papadopoulos, B. Vogelstein, K.W. Kinzler, V.E. Velculescu, The consensus coding sequences of human breast and colorectal cancers, Science 314 (2006) 268–274.
[6] V. Torchilin, Tumor delivery of macromolecular drugs based on the EPR effect, Adv. Drug Deliv. Rev. 63 (2011) 131–135.
[7] Y. Matsumura, H. Maeda, A new concept for macromolecular therapeutics in cancer chemotherapy: mechanism of tumoritropic accumulation of proteins and the antitumor agent SMANCS, Cancer Res. 46 (1986) 6387–6392.
[8] H. Maeda, The enhanced permeability and retention (EPR) effect in tumor vasculature: the key role of tumor-selective macromolecular drug targeting, in: G. Weber (Ed.), Advances in Enzyme Regulation, Elsevier Science Ltd, Oxford, 2001, pp. 189–207.
[9] H. Maeda, SMANCS and polymer-conjugated macromolecular drugs: advantages in cancer chemotherapy, Adv. Drug Deliv. Rev. 46 (2001) 169–185.
[10] J. Fang, T. Sawa, H. Maeda, Factors and mechanism of "EPR" effect and the enhanced antitumor effects of macromolecular drugs including SMANCS, Adv. Exp. Med. Biol. 519 (2003) 29–49.
[11] T. Seki, J. Fang, H. Maeda, Tumor targeted macromolecular drug delivery based on the enhanced permeability and retention effect in solid tumor, in: Y. Lu, R.I. Mahato (Eds.), Pharmaceutical Perspectives of Cancer Therapeutics, Springer Publishing Co., New York, 2009, pp. 93–120.
[12] H. Maeda, G.Y. Bharate, J. Daruwalla, Polymeric drugs and nanomedicines for efficient tumor targeted drug delivery based on EPR-effect, Eur. J. Pharm. Biopharm. 71 (2009) 409–419.
[13] H. Maeda, K. Greish, J. Fang, The EPR effect and polymeric drugs: a paradigm shift for cancer chemotherapy in the 21st century, Adv. Polym. Sci. 193 (2006) 103–121.
[14] A.K. Iyer, K. Greish, J. Fang, H. Maeda, Exploiting the enhanced permeability and retention effect for tumor targeting, Drug Discov. Today 11 (2006) 812–818.
[15] M.J. Vicent, H. Ringsdorf, R. Duncan, Polymer therapeutics: clinical applications and challenges for development, Adv. Drug Deliv. Rev. 61 (2009) 1117–1120.
[16] R. Duncan, The dawning era of polymer therapeutics, Nat. Rev. Drug Discov. 2 (2003) 347–360.
[17] Y. Matsumura, K. Kataoka, Preclinical and clinical studies of anticancer agent-incorporating polymer micelles, Cancer Sci. 100 (2009) 572–579.
[18] S. Maki, T. Konno, H. Maeda, Image enhancement in computerized tomography for sensitive diagnosis of liver cancer and semiquantitation of tumor selective drug targeting with oily contrast medium, Cancer 56 (1985) 751–757.
[19] A. Nagamitsu, K. Greish, H. Maeda, Elevating blood pressure as a strategy to increase tumor-targeted delivery of macromolecular drug SMANCS: cases of advanced solid tumors, Jpn. J. Oncol. 39 (2009) 756–766.
[20] H. Maeda, J. Takeshita, R. Kanamaru, A lipophilic derivative of neocarzinostatin. A polymer conjugation of an antitumor protein antibiotic, Int. J. Pept. Protein Res. 14 (1979) 81–87.
[21] H. Maeda, T. Matsumoto, T. Konon, K. Iwaki, M. Ueda, Tailor-making of protein drugs by polymer conjugation for tumor targeting: a brief review on smancs, J. Protein Chem. 3 (1984) 181–193.
[22] H. Maeda, Y. Matsumura, T. Oda, K. Sasamoto, Cancer selective macromolecular therapeutics: tailoring of an antitumor protein drug, in: R.E. Feeney, J.R. Whitaker (Eds.), Protein Tailoring for Food and Medical Uses, Marcel Dekker, New York, 1983, pp. 353–382.
[23] J. Fang, T. Sawa, T. Akaike, H. Maeda, Tumor-targeted delivery of polyethylene glycol-conjugated D-amino acid oxidase for antitumor therapy via enzymatic generation of hydrogen peroxide, Cancer Res. 62 (2002) 3138–3143.
[24] J. Fang, T. Sawa, T. Akaike, T. Akuta, S.K. Sahoo, K. Greish, A. Hamada, H. Maeda, *In vivo* antitumor activity of pegylated zinc protoporphyrin: targeted inhibition of heme oxygenase in solid tumor, Cancer Res. 63 (2003) 3567–3674.
[25] A.K. Iyer, K. Greish, J. Fang, R. Murakami, H. Maeda, High-loading nanosized micelles of copoly(styrene-maleic acid)-zinc protoporphyrin for targeted delivery of a potent heme oxygenase inhibitor, Biomaterials 28 (2007) 1871–1881.
[26] K. Greish, A. Nagamitsu, J. Fang, H. Maeda, Copoly(styrene-maleic acid)-pirarubicin micelles: high tumor-targeting efficiency with little toxicity, Bioconjug. Chem. 16 (2005) 230–236.
[27] K. Greish, T. Sawa, J. Fang, T. Akaike, H. Maeda, SMA-doxorubicin, a new polymeric micellar drug for effective targeting to solid tumours, J. Control. Release 97 (2004) 219–230.
[28] H. Maeda, Y. Matsumura, Tumoritropic and lymphotropic principles of macromolecular drugs, Crit. Rev. Ther. Drug Carrier Syst. 6 (1989) 193–210.
[29] K. Greish, J. Fang, T. Inutsuka, A. Nagamitsu, H. Maeda, Macromolecular therapeutics: advantages and prospects with special emphasis on solid tumor targeting, Clin. Pharmacokinet. 42 (2003) 1089–1105.
[30] T. Konno, H. Maeda, K. Iwai, S. Maki, S. Tashiro, M. Uchida, Y. Miyauchi, Selective targeting of anti-cancer drug and simultaneous image enhancement in solid tumors by arterially administered lipid contrast medium, Cancer 54 (1984) 2367–2374.
[31] H. Maeda, T. Sawa, T. Konno, Mechanism of tumor-targeted delivery of macromolecular drugs, including the EPR effect in solid tumor and clinical overview of the prototype polymeric drug SMANCS, J. Control. Release 74 (2001) 47–61.
[32] Y. Noguchi, J. Wu, R. Duncan, J. Strohalm, K. Ulbrich, T. Akaike, H. Maeda, Early phase tumor accumulation of macromolecules: a great difference in clearance rate between tumor and normal tissues, Jpn. J. Cancer Res. 89 (1998) 307–314.
[33] L.W. Seymour, Y. Miyamoto, H. Maeda, M. Brereton, J. Strohalm, K. Ulbrich, R. Duncan, Influence of molecular weight on passive tumour accumulation of a soluble macromolecular drug carrier, Eur. J. Cancer 31A (1995) 766–770.
[34] M. Zhao, M. Yang, X.M. Li, P. Jiang, E. Baranov, S. Li, M. Xu, S. Penman, R.M. Hoffman, Tumor-targeting bacterial therapy with amino acid auxotrophs of

GFP-expressing *Salmonella typhimurium*, Proc. Natl. Acad. Sci. U. S. A. 102 (2005) 755–760.
[35] M. Zhao, M. Yang, H. Ma, X. Li, X. Tan, S. Li, Z. Yang, R.M. Hoffman, Targeted therapy with a *Salmonella typhimurium* leucine-arginine auxotroph cures orthotopic human breast tumors in nude mice, Cancer Res. 66 (2006) 7647–7652.
[36] R.M. Hoffman, Tumor-targeting amino acid auxotrophic *Salmonella typhimurium*, Amino Acids 37 (2009) 509–521.
[37] T. Sawa, J. Wu, T. Akaike, H. Maeda, Tumor-targeting chemotherapy by a xanthine oxidase-polymer conjugate that generates oxygen-free radicals in tumor tissue, Cancer Res. 60 (2000) 666–671.
[38] R.B. Campbell, D. Fukumura, E.B. Brown, L.M. Mazzola, Y. Izumi, R.K. Jain, V.P. Torchilin, L.L. Munn, Cationic charge determines the distribution of liposomes between the vascular and extravascular compartments of tumors, Cancer Res. 62 (2002) 6831–6836.
[39] M. Nakamura, P. Davila-Zavala, H. Tokuda, Y. Takakura, M. Hashida, Uptake and gene expression of naked plasmid DNA in cultured brain microvessel endothelial cells, Biochem. Biophys. Res. Commun. 245 (1998) 235–239.
[40] S.D. Li, L. Huang, Pharmacokinetics and biodistribution of nanoparticles, Mol. Pharm. 5 (2008) 496–504.
[41] D.E. Keyler, P.R. Pentel, D.B. Haughey, Pharmacokinetics and toxicity of high-dose human α_1-acid glycoprotein infusion in the rat, J. Pharm. Sci. 76 (2006) 101–104.
[42] G. Gregoriadis, Liposome research in drug delivery: the early days, J. Drug Target. 16 (2008) 520–524.
[43] T.M. Allen, C. Hansen, F. Martin, C. Redemann, A. Yau-Young, Liposomes containing synthetic lipid derivatives of poly(ethylene glycol) show prolonged circulation half-lives in vivo, Biochim. Biophys. Acta 1066 (1991) 29–36.
[44] M.L. Immordino, F. Dosio, L. Cattel, Stealth liposomes: review of the basic science, rationale, and clinical applications, existing and potential, Int. J. Nanomed. 1 (2006) 297–315.
[45] D.E. Owens III, N.A. Peppas, Opsonization, biodistribution, and pharmacokinetics of polymeric nanoparticles, Int. J. Pharm. 307 (2006) 93–102.
[46] S.D. Li, L. Huang, Surface-modified LPD nanoparticles for tumor targeting, Ann. N.Y. Acad. Sci. 1082 (2006) 1–8.
[47] T. Ishida, M. Ichihara, X. Wang, K. Yamamoto, J. Kimura, E. Majima, H. Kiwada, Injection of PEGylated liposomes in rats elicits PEG-specific IgM, which is responsible for rapid elimination of a second dose of PEGylated liposomes, J. Control. Release 112 (2006) 15–25.
[48] T. Ishida, H. Kiwada, Accelerated blood clearance (ABC) phenomenon upon repeated injection of PEGylated liposomes, Int. J. Pharm. 354 (2008) 56–62.
[49] H. Hatakeyama, H. Akita, K. Kogure, M. Oishi, Y. Nagasaki, Y. Kihira, M. Ueno, H. Kobayashi, H. Kikuchi, H. Harashima, Development of a novel systemic gene delivery system for cancer therapy with a tumor-specific cleavable PEG-lipid, Gene Ther. 14 (2007) 68–77.
[50] T. Masuda, H. Akita, K. Niikura, T. Nishio, M. Ukawa, K. Enoto, R. Danev, K. Nagayama, K. Ijiro, H. Harashima, Envelope-type lipid nanoparticles incorporating a short PEG-lipid conjugate for improved control of intracellular trafficking and transgene transcription, Biomaterials 27 (2009) 4806–4814.
[51] H. Nakamura, H. Maeda, Intracellular Uptake of Water Soluble ZnPP Micelles (SMA-ZnPP and PEG-ZnPP) and the Unique Release Mechanism of the Drug from Their Micelles, The 37th Annual Meeting and Exposition of the Controlled Release Society, Portland, USA, July 10–14, 2010.
[52] T.R. Daniels, T. Delgado, G. Helguera, M.L. Penichet, The transferrin receptor part II: targeted delivery of therapeutic agents into cancer cells, Clin. Immunol. 121 (2006) 159–176.
[53] S. Sundaram, S.K. Roy, B.K. Ambati, U.B. Kompella, Surface-functionalized nanoparticles for targeted gene delivery across nasal respiratory epithelium, FASEB J. 23 (2009) 3752–3765.
[54] X. Yang, C.G. Koh, S. Liu, X. Pan, R. Santhanam, B. Yu, Y. Peng, J. Pang, S. Golan, Y. Talmon, Y. Jin, N. Muthusamy, J.C. Byrd, K.K. Chan, L.J. Lee, G. Marcucci, R.J. Lee, Transferrin receptor-targeted lipid nanoparticles for delivery of an antisense oligodeoxyribonucleotide against Bcl-2, Mol. Pharm. 6 (2009) 221–230.
[55] M. Taketani, M. Shii, K. Ohura, S. Ninomiya, T. Imai, Carboxylesterase in the liver and small intestine of experimental animals and human, Life Sci. 81 (2007) 924–932.
[56] J. Folkman, Tumor angiogenesis in cancer, therapeutic implications, N. Engl. J. Med. 285 (1971) 1182–1186.
[57] J. Folkman, Angiogenesis in cancer, vascular, rheumatoid and other diseases, Nat. Med. 1 (1995) 27–31.
[58] J. Folkman, What is the evidence that tumors are angiogenesis dependent? J. Natl. Cancer Inst. 82 (1990) 4–6.
[59] J. Daruwalla, K. Greish, C. Malcontenti-Wilson, V. Muralidharan, A. Iyer, H. Maeda, C. Christophi, Styrene maleic acid-pirarubicin disrupts tumor microcirculation and enhances the permeability of colorectal liver metastases, J. Vasc. Res. 46 (2009) 218–228.
[60] H. Maeda, J. Fang, T. Inutsuka, Y. Kitamoto, Vascular permeability enhancement in solid tumor: various factors, mechanisms involved and its implications, Int. Immunopharmacol. 3 (2003) 319–328.
[61] K. Hori, M. Suzuki, S. Tanda, S. Saito, M. Shinozaki, Q.H. Zhang, Fluctuations in tumor blood flow under normotension and the effect of angiotensin II-induced hypertension, Jpn. J. Cancer Res. 82 (1991) 1309–1316.
[62] M. Suzuki, K. Hori, Z. Abe, S. Asito, H. Sato, A new approach to cancer chemotherapy: selective enhancement of tumor blood flow with angiotensin II, J. Natl. Cancer Inst. 67 (1981) 663–669.
[63] S. Skinner, P. Tutton, P. O'Brien, Microvascular architecture of experimental colon tumors in the rat, Cancer Res. 50 (1990) 2411–2417.
[64] M. Suzuki, T. Takahashi, T. Sato, Medial regression and its functional significance in tumor-supplying host arteries, Cancer 59 (1987) 444–450.
[65] K. Greish, A.K. Iyer, J. Fang, M. Kawasuji, H. Maeda, Enhanced permeability and retention (EPR) effect and tumor-selective delivery of anticancer drugs, in: V.P. Torchilin (Ed.), Delivery of Protein and Peptide Drugs in Cancer, Imperial College Press, London, 2006, pp. 37–52.
[66] K. Hori, S. Saito, H. Takahashi, H. Sato, H. Maeda, Y. Sato, Tumor-selective blood flow decrease induced by an angiotensin converting enzyme inhibitor, temocapril hydrochloride, Jpn. J. Cancer Res. 91 (2000) 261–269.
[67] K. Iwai, H. Maeda, T. Konno, Use of oily contrast medium for selective drug targeting to tumor: enhanced therapeutic effect and X-ray image, Cancer Res. 44 (1984) 2115–2121.
[68] T. Konno, Targeting chemotherapy for hepatoma: arterial administration of anticancer drugs dissolved in Lipiodol, Eur. J. Cancer 28 (1992) 403–409.
[69] H. Maeda, J. Takeshita, A. Yamashita, Lymphotropic accumulation of an antitumor antibiotic protein, neocarzinostatin, Eur. J. Cancer 16 (1980) 723–731.
[70] H. Maeda, J. Takeshita, R. Kanamaru, H. Sato, J. Katoh, H. Sato, Antimetastatic and antitumor activity of a derivative of neocarzinostatin: an organic solvent- and water-soluble polymer-conjugated protein, Gann 70 (1979) 601–606.
[71] K. Yamasaki, T. Konno, Y. Miyauchi, H. Maeda, Reduction of hepatic metastases in rabbits by administration of an oily anticancer agent into the portal vein, Cancer Res. 47 (1987) 852–855.
[72] N. Ohtsuka, T. Konno, Y. Miyauchi, H. Maeda, Anticancer effects of arterial administration of the anticancer agent SMANCS with lipiodol on metastatic lymph nodes, Cancer 59 (1987) 1560–1565.
[73] H. Maeda, Y. Masumura, H. Kato, Purification and identification of [hydroxyprolyl^3]bradykinin in ascitic fluid from a patient with gastric cancer, J. Biol. Chem. 263 (1988) 16,051–16,054.
[74] Y. Matsumura, M. Kimura, T. Yamamoto, H. Maeda, Involvement of the kinin-generating cascade in enhanced vascular permeability in tumor tissue, Jpn. J. Cancer Res. 79 (1988) 1327–1334.
[75] Y. Matsumura, K. Maruo, M. Kumara, T. Yamamoto, T. Konno, H. Maeda, Kinin-generating cascade in advanced cancer patients and in vitro study, Jpn. J. Cancer Res. 82 (1991) 732–741.
[76] J. Wu, T. Akaike, H. Maeda, Modulation of enhanced vascular permeability in tumors by a bradykinin antagonist, a cyclooxygenase inhibitor, and a nitric oxide scavenger, Cancer Res. 58 (1998) 159–165.
[77] K. Doi, T. Akaike, H. Horie, Y. Noguchi, S. Fujii, T. Beppu, M. Ogawa, H. Maeda, Excessive production of nitric oxide in rat solid tumor and its implication in rapid tumor growth, Cancer 77 (1996) 1598–1604.
[78] H. Maeda, Y. Noguchi, K. Sato, T. Akaike, Enhanced vascular permeability in solid tumor is mediated by nitric oxide and inhibited by both nitric oxide scavenger and nitric oxide synthase inhibitor, Jpn. J. Cancer Res. 85 (1994) 331–334.
[79] J. Wu, T. Akaike, K. Hayashida, T. Okamoto, A. Okuyama, H. Maeda, Enhanced vascular permeability in solid tumor involving peroxynitrite and matrix metalloproteinases, Jpn. J. Cancer Res. 92 (2001) 439–451.
[80] H.R. Reichman, C.L. Farrell, F.R. Del Maestro, Effect of steroids and nonsteroid anti-inflammatory agents on vascular permeability in a rat glioma model, J. Neurosurg. 65 (1986) 233–237.
[81] D.R. Senger, S.J. Galli, A.M. Dovorak, C.A. Perruzzi, V.S. Harvey, H.F. Dvorak, Tumor cells secrete a vascular permeability factor that promotes accumulation of ascites fluid, Science 219 (1983) 983–985.
[82] N. Ferrara, W.J. Henzel, Pituitary follicular cells secrete a novel heparin-binding growth factor specific for vascular endothelial cells, Biochem. Biophys. Res. Commun. 161 (1989) 851–858.
[83] R.A. Rosenthal, J.F. Megyesi, W.J. Henzel, N. Ferrara, J. Folkman, Conditioned medium from mouse sarcoma 180 cells contains vascular endothelial growth factor, Growth Factors 4 (1990) 53–59.
[84] D.W. Leung, G. Cachianes, W.-J. Kuang, D.V. Goeddel, N. Ferrara, Vascular endothelial growth factor is a secreted angiogenic mitogen, Science 246 (1989) 1306–1309.
[85] P.J. Keck, S.D. Hauser, G. Krivi, K. Sanzo, T. Warren, J. Feder, D.T. Connolly, Vascular permeability factor, an endothelial cell mitogen related to PDGF, Science 246 (1989) 1309–1312.
[86] M.R. Kano, Y. Komuta, C. Iwata, M. Oka, Y.T. Shirai, Y. Morishita, Y. Ouchi, K. Kataoka, K. Miyazono, Comparison of the effects of the kinase inhibitors imatinib, sorafenib, and transforming growth factor-β receptor inhibitor on extravasation of nanoparticles from neovasculature, Cancer Sci. 100 (2009) 173–180.
[87] M. Del Rosso, G. Fibbi, M. Pucci, F. Margheri, S. Serrati, The plasminogen activation system in inflammation, Front. Biosci. 13 (2008) 4667–4686.
[88] H. Maeda, J. Wu, T. Okamoto, K. Maruo, T. Akaike, Kallikrein–kinin in infection and cancer, Immunopharmacology 43 (1999) 115–128.
[89] J. Wu, T. Akaike, K. Hayashida, Y. Miyamoto, T. Nakagawa, K. Miyakawa, W. Müller-Esterl, H. Maeda, Identification of bradykinin receptors in clinical cancer specimens and murine tumor tissues, Int. J. Cancer 98 (2002) 29–35.
[90] K.D. Bhoola, C.D. Figueroa, K. Worthy, Bioregulation of kinins: kallikreins, kininogens, and kininases, Pharmacol. Rev. 44 (1992) 1–80.
[91] K. Bhoola, R. Ramsaroop, J. Plendl, B. Cassim, Z. Dlamini, S. Naicker, Kallikrein and kinin receptor expression in inflammation and cancer, Biol. Chem. 382 (2001) 77–89.
[92] R. Kou, D. Greif, T. Michel, Dephosphorylation of endothelial nitric-oxide synthase by vascular endothelial growth factor. Implications for the vascular responses to cyclosporine A, J. Biol. Chem. 277 (2002) 29,669–29,673.
[93] K. Doi, T. Akaike, S. Fujii, S. Tanaka, N. Ikebe, T. Beppu, S. Shibahara, M. Ogawa, H. Maeda, Induction of haem oxygenase-1 by nitric oxide and ischaemia in

experimental solid tumours and implications for tumour growth, Br. J. Cancer 80 (1999) 1945–1954.
[94] L.R. Kisley, B.S. Barrett, A.K. Bauer, L.D. Dwyer-Nield, B. Barthel, A.M. Meyer, D.C. Thompson, A.M. Malkinson, Genetic ablation of inducible nitric oxide synthase decreases mouse lung tumorigenesis, Cancer Res. 62 (2002) 6850–6856.
[95] J.S. Beckman, T.W. Beckman, J. Chen, P.A. Marshall, B.A. Freeman, Apparent hydroxyl radical production by peroxynitrite: implications for endothelial injury from nitric oxide and superoxide, Proc. Natl. Acad. Sci. U. S. A. 87 (1990) 1620–1624.
[96] J.S. Beckman, W.H. Koppenol, Nitric oxide, superoxide, and peroxynitrite: the good, the bad, and ugly, Am. J. Physiol. 271 (1996) C1424–C1437.
[97] T. Akaike, H. Maeda, Nitric oxide and virus infection, Immunology 101 (2000) 300–308.
[98] T. Akaike, H. Maeda, Pathophysiological effects of high-output production of nitric oxide, in: L.J. Ignarro (Ed.), Nitric Oxide: Biology and Pathobiology, Academic Press, San Diego, CA, 2000, pp. 733–745.
[99] T. Akaike, M. Suga, H. Maeda, Free radicals in viral pathogenesis: molecular mechanisms involving superoxide and NO, Proc. Soc. Exp. Biol. Med. 217 (1998) 64–73.
[100] H. Maeda, T. Sawa, T. Yubisui, T. Akaike, Free radical generation from heterocyclic amines by cytochrome b5 reductase in the presence of NADH, Cancer Lett. 143 (1999) 117–121.
[101] T. Sawa, T. Akaike, K. Ichimori, T. Akuta, K. Kaneko, H. Nakayama, D.J. Stuehr, H. Maeda, Superoxide generation mediated by 8-nitroguanosine, a highly redox-active nucleic acid derivative, Biochem. Biophys. Res. Commun. 311 (2003) 300–306.
[102] T. Okamoto, T. Akaike, T. Nagano, S. Miyajima, M. Suga, M. Ando, K. Ichinori, H. Maeda, Activation of human neutrophil procollagenase by nitrogen dioxide and peroxynitrite: a novel mechanism for procollagenase activation involving nitric oxide, Arch. Biochem. Biophys. 342 (1997) 261–274.
[103] H. Kuwahara, T. Kariu, J. Fang, H. Maeda, Generation of drug-resistant mutants of *Helicobacter pylori* in the presence of peroxynitrite, a derivative of nitric oxide, at pathophysiological concentration, Microbiol. Immunol. 53 (2009) 1–7.
[104] I. Massova, L.P. Korta, R. Fridman, S. Mobashery, Matrix metalloproteinases: structures, evolution, and diversification, FASEB J. 12 (1998) 1075–1095.
[105] B.P. Himelstein, R. Canete-Soler, E.J. Bernhard, D.W. Dilks, R.J. Muschel, Metalloproteinases in tumor progression: the contribution of MMP-9, Invasion Metastasis 14 (1994–1995) 246–258.
[106] A.F. Chambers, L.M. Matrisian, Changing views of the role of matrix metalloproteinases in metastasis, J. Natl. Cancer Inst. 89 (1997) 1260–1270.
[107] J. Yoneda, H. Kuniyasu, M.A. Crispens, J.E. Price, C.D. Bucana, I.J. Fidler, Expression of angiogenesis-related genes and progression of human ovarian carcinomas in nude mice, J. Natl. Cancer Inst. 90 (1998) 447–454.
[108] T. Sawa, M.H. Zaki, T. Okamoto, T. Akuta, Y. Tokutomi, S. Kim-Mitsuyama, H. Ihara, A. Kobayashi, M. Yamamoto, S. Fujii, H. Arimoto, T. Akaike, Protein S-guanylation by the biological signal 8-nitroguanosine 3′, 5′-cyclic monophosphate, Nat. Chem. Biol. 3 (2007) 727–735.
[109] N. Chand, P. Eyre, Bradykinin relaxes contracted airways through prostaglandin production, J. Pharm. Pharmacol. 29 (1977) 387–388.
[110] I. Furuta, H. Yamada, T. Sagawa, S. Fujimoto, Effects of inflammatory cytokines on prostaglandin E_2 production from human amnion cells cultured in serum-free condition, Gynecol. Obstet. Invest. 49 (2000) 93–97.
[111] S. Tanaka, T. Akaike, J. Wu, J. Fang, T. Sawa, M. Ogawa, T. Beppu, H. Maeda, Modulation of tumor-selective vascular blood flow and extravasation by the stable prostaglandin I_2 analogue beraprost sodium, J. Drug Target. 11 (2003) 45–52.
[112] A. Grothey, E. Galanis, Targeting angiogenesis: progress with anti-VEGF treatment with large molecules, Nat. Rev. Clin. Oncol. 6 (2009) 507–518.
[113] H.F. Dvorak, L.F. Brown, M. Detmar, A.M. Dvorak, Vascular permeability factor/vascular endothelial growth factor, microvascular hyperpermeability, and angiogenesis, Am. J. Pathol. 146 (1995) 1029–1039.
[114] T. Murohara, J.R. Horowitz, M. Silver, Y. Tsurumi, D. Chen, A. Sullivan, J.M. Isner, Vascular endothelial growth factor/vascular permeability factor enhances vascular permeability via nitric oxide and prostacyclin, Circulation 97 (1998) 99–107.
[115] A. Papapetropoulos, G. García-Cardeña, J.A. Madri, W.C. Sessa, Nitric oxide production contributes to the angiogenic properties of vascular endothelial growth factor in human endothelial cells, J. Clin. Invest. 100 (1997) 3131–3139.
[116] C.J. Li, Y. Miyamoto, Y. Kojima, H. Maeda, Augmentation of tumor delivery of macromolecular drugs with reduced bone marrow delivery by elevating blood pressure, Br. J. Cancer 67 (1993) 975–980.
[117] B.F. Jordan, P.D. Misson, R. Demeure, C. Baudelet, N. Beghein, B. Gallez, Changes in tumor oxygenation/perfusion induced by the NO donor, isosorbide dinitrate, in comparison with carbogen: monitoring by EPR and MRI, Int. J. Radiat. Oncol. Biol. Phys. 48 (2000) 565–570.
[118] J.B. Mitchell, D.A. Wink, W. DeGraff, J. Gamson, L.K. Keefer, M.C. Krishna, Hypoxic mammalian cell radiosensitization by nitric oxide, Cancer Res. 53 (1993) 5845–5848.
[119] J.M. Fukuto, J.Y. Cho, C.H. Switzer, The chemical properties of nitric oxide and related nitrogen oxides, in: L.J. Ignarro (Ed.), Nitric Oxide: Biology and Pathobiology, Academic Press, San Diego, CA, 2000, pp. 23–39.
[120] M. Feelisch, E.A. Noack, Correlation between nitric oxide formation during degradation of organic nitrates and activation of guanylate cyclase, Eur. J. Pharmacol. 139 (1987) 19–30.
[121] T. Seki, J. Fang, H. Maeda, Enhanced delivery of macromolecular antitumor drugs to tumors by nitroglycerin application, Cancer Sci. 100 (2009) 2426–2430 available online, doi:10.1111/j.1349-7006.2009.01323.x.
[122] H. Kojima, Y. Urano, K. Kikuchi, T. Higuchi, Y. Hirata, T. Nagano, Fluorescent indicators for imaging nitric oxide production, Angew. Chem. Int. Ed. Engl. 38 (1999) 3209–3212.
[123] G. Pasut, F. Greco, A. Mero, R. Mendichi, C. Fante, R.J. Green, F.M. Veronese, Polymer–drug conjugates for combination anticancer therapy: investigating the mechanism of action, J. Med. Chem. 52 (2009) 6499–6502.
[124] L. Santucci, A. Mencarelli, B. Renga, G. Pasut, F. Veronese, A. Zacheo, A. Germani, S. Fiorucci, Nitric oxide modulates proapoptotic and antiapoptotic properties of chemotherapy agents: the case of NO-pegylated epirubicin, FASEB J. 20 (2006) 765–767.
[125] L. Santucci, A. Mencarelli, B. Renga, D. Ceccobelli, G. Pasut, F.M. Veronese, E. Distrutti, S. Fiorucci, Cardiac safety and antitumoral activity of a new nitric oxide derivative of pegylated epirubicin in mice, Anticancer Drugs 18 (2007) 1081–1091.
[126] H. Yasuda, M. Yamaya, K. Nakayama, T. Sasaki, S. Ebihara, A. Kanda, M. Asada, D. Inoue, T. Suzuki, T. Okazaki, H. Takahashi, M. Yoshida, T. Kaneta, K. Ishizawa, S. Yamanda, N. Tomita, M. Yamasaki, A. Kikuchi, H. Kubo, H. Sasaki, Randomized phase II trial comparing nitroglycerin plus vinorelbine and cisplatin with vinorelbine and cisplatin alone in previously untreated stage IIIB/IV non-small cell lung cancer, J. Clin. Oncol. 24 (2006) 688–694.
[127] H. Yasuda, K. Nakayama, M. Watanabe, S. Suzuki, H. Fuji, S. Okinaga, A. Kanda, K. Zayazu, T. Sasaki, M. Asada, T. Suzuki, M. Yoshida, S. Yamanda, D. Inoue, T. Kaneta, T. Kondo, Y. Takai, H. Sasaki, K. Yanagihara, M. Yamaya, Nitroglycerin treatment may increase response to docetaxel and carboplatin regimen via inhibitions of hypoxia-inducible factor-1 pathway and P-glycoprotein in patients with lung adenocarcinoma, Clin. Cancer Res. 12 (2006) 6748–6757.
[128] H. Yasuda, K. Yanagihara, K. Nakayama, T. Mio, T. Sasaki, M. Asada, M. Yamaya, M. Fukushima, Therapeutic applications of nitric oxide for malignant tumor in animal models and human studies, in: B. Bonavida (Ed.), Nitric Oxide and Cancer, Springer Science, New York, 2009.
[129] D.R. Siemens, J.P.W. Heaton, M.A. Adams, J. Kawakami, C.H. Graham, Phase II study of nitric oxide donor for men with increasing prostate-specific antigen level after surgery or radiotherapy for prostate cancer, Urology 74 (2009) 878–883.
[130] T. Akaike, M. Yoshida, Y. Miyamoto, K. Sato, M. Kohno, K. Sasamoto, K. Miyazaki, S. Ueda, H. Maeda, Antagonistic action of imidazolineoxyl N-oxides against endothelium-derived relaxing factor/.NO through a radical reaction, Biochemistry 32 (1993) 827–832.
[131] A. Noguchi, T. Takahashi, T. Yamaguchi, K. Kitamura, A. Noguchi, H. Tsurumi, K. Takashina, H. Maeda, Enhanced tumor localization of monoclonal antibody by treatment with kinase II inhibitor and angiotension II, Jpn. J. Cancer Res. 83 (1992) 240–243.

Journal of Controlled Release 155 (2011) 367–375

Contents lists available at ScienceDirect

Journal of Controlled Release

journal homepage: www.elsevier.com/locate/jconrel

Intracellular uptake and behavior of two types zinc protoporphyrin (ZnPP) micelles, SMA-ZnPP and PEG-ZnPP as anticancer agents; unique intracellular disintegration of SMA micelles

Hideaki Nakamura [a], Jun Fang [a], Bharate Gahininath [a,b], Kenji Tsukigawa [a,b], Hiroshi Maeda [a,b,*]

[a] Laboratory of Microbiology and Oncology, Faculty of Pharmaceutical Science, Sojo University, Ikeda 4-22-1, Kumamoto 860-0082, Japan
[b] Department of Applied Chemistry, Sojo University, Ikeda 4-22-1, Kumamoto 860-0082, Japan

ARTICLE INFO

Article history:
Received 7 January 2011
Accepted 26 April 2011
Available online 9 May 2011

Keyword:
HO-1 inhibitor
HSP32
Anticancer micelles
SMA-ZnPP
PEG-ZnPP

ABSTRACT

SMA-ZnPP and PEG-ZnPP are micellar drugs, encapsulating zinc protoporphyrin IX (ZnPP) with styrene maleic acid copolymer (SMA) and covalent conjugate of ZnPP with polyethylene glycol (PEG) respectively. Their intracellular uptake rate and subcellular localization were investigated. We found SMA-ZnPP showed higher and more efficient (about 2.5 times) intracellular uptake rate than PEG-ZnPP, although both SMA-ZnPP and PEG-ZnPP micelles were localized at endoplasmic reticulum (ER) and inhibited the target enzyme heme oxygenase 1 (HO-1) similarly. Both micellar ZnPP were taken up into the tumor cells by endocytosis. Furthermore SMA-ZnPP and PEG-ZnPP were examined for their drug releasing mechanisms. Liberation of ZnPP from the SMA micelle appears to depend on cellular amphiphilic components such as lecithin, while that for PEG-ZnPP depends on hydrolytic cleavage. These results indicate that these micelle formulations make water insoluble ZnPP to water soluble practical anticancer agents.

1. Introduction

Heme oxygenase-1 (HO-1), also known as heat shock protein 32 (HSP 32), is a stress related protein, that is involved in cellular defense against oxystress. HO-1 is induced by various stimuli such as ultraviolet radiation, oxidative stimuli, metalloporphyrins, heavy metals, nitric oxide and the others [1–4]. This phenomenon is ubiquitously seen in mammalian cells including normal cells and cancer cells. It is intriguing that most cancer cells lack cellular defense systems against oxidative stress such as catalase, superoxide dismutase, glutathione peroxidase and the others. Alternatively cancer cells rely on either HO-1 alone or with glutathione S-transferase against oxystress for survival by defending cells [5,6]. Under these circumstances, it was reported that inhibition or suppression of HO-1 activity by a specific inhibitor or siRNA leads to cancer selective cell death [7–9]. It was also reported that enzymatic activity of HO-1 seemed to be located at the endoplasmic reticulum (ER) in cells and anchored via the single transmembrane peptide segment located at the C-terminus of HO-1 protein [10].

In zinc protoporphyrin (ZnPP), zinc atom is coordinated in the center of protoporphyrin IX, and we found that ZnPP becomes one of the specific inhibitors against HO-1 and exhibits a cytotoxic effect against various cancer cells [8,9,11]. However water insoluble property of ZnPP hampers its therapeutic application. To solve this problem we have developed water soluble ZnPP derivatives, polyethylene glycol (PEG) conjugated ZnPP (PEG-ZnPP) and ZnPP encapsulated with styrene maleic acid copolymer (SMA) micelle (SMA-ZnPP) (Fig. 1A and B) [9,11]. PEG-ZnPP and SMA-ZnPP micelles were exhibited to have mean particle size of around 180 nm and 50 nm, respectively. These biocompatible macromolecular drugs in general, for example SMANCS (SMA-neocarzinostatin), SMA-THP (SMA-pirarubicin) micelle, PEG-DAO (PEG-conjugated D-amino acid oxidase), SMA-AHPP (4-amino −6-hydroxypyrazolo[3,4-d]pyrimidine SMA conjugate) and the other tend to accumulate preferentially at tumor site by the mechanism called enhanced permeability and retention (EPR) effect [12–18].

Most macromolecular drugs are transported into cells by active transport mechanisms, namely, endocytosis [19–22], where clathrin dependent, caveolae mediated and fluid phase endocytosis pathways are well known in the endocytosis pathway of eukaryotic cells, as a common cellular internalization pathway of macromolecular drugs. Cellular internalization is the critical step to exert therapeutic effect, where both receptor dependent and independent endocytosis are well investigated for macromolecular drugs. So far, to facilitate the cellular uptake of macromolecular drugs, or to increase selectivity to target cancer cells, the specific tissues, or specific receptors for such as transferin, asialoglycoprotein, folate, epidermal growth factor and chemokine, are frequently utilized [23–25].

Cellular internalization of SMA-micells or the PEG-ZnPP conjugates, and further delivery of free ZnPP to specific intracellular target

* Corresponding author at: Laboratory of Microbiology and Oncology, Faculty of Pharmaceutical Science, Sojo University, Ikeda 4-22-1, Kumamoto 860-0082, Japan. Tel.: +81 96 326 4114; fax: +81 096 326 3185.
E-mail address: hirmaeda@ph.sojo-u.ac.jp (H. Maeda).

0168-3659/$ – see front matter © 2011 Elsevier B.V. All rights reserved.
doi:10.1016/j.jconrel.2011.04.025

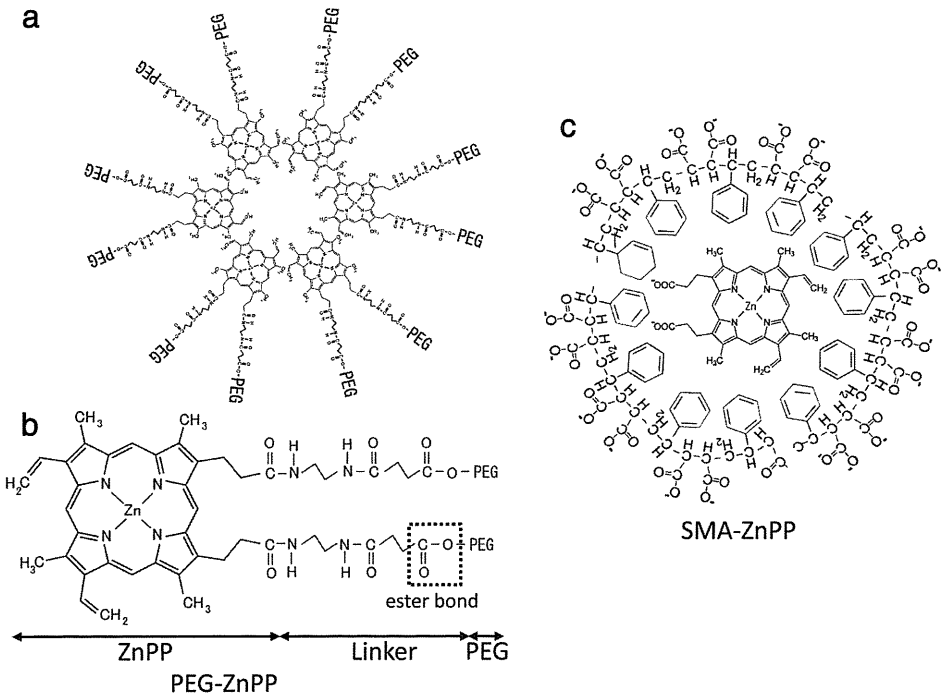

Fig. 1. In (a), hydrophobic ZnPP heads clustered and PEG chain tails with hydrophilic property extend outward direction in contact with water. (b) depicts each component of PEG-ZnPP (c) styrene residue of hydrophobic nature clustered and encapsulating ZnPP inside. Poly carboxylate groups and facing toward water.

molecules is the critical steps to exert cytotoxicity, since ZnPP is a competitive inhibitor of HO-1. Therefore its access to HO-1 molecules needs to be elucidated. In this study, we investigated the intracellular fate of PEG-ZnPP and SMA-ZnPP micelles focusing on the mode of internalization, subcellular localization and uncoating process of micelles. Different mechanisms of ZnPP release from each micelle were found to undergo at molecular level in the tissue and at the cellular levels.

2. Materials and methods

2.1. Materials

Protoporphyrin IX (PP) and antibiotics (penicillin and streptomycin) were obtained from Sigma Aldrich Chemical Co., St. Louis, MO. Free ZnPP was obtained from Frontier Scientific, Inc., Salt Lake, Utah. SMA (maleic anhydride form) (mean mol wt. ≈ 1600) was obtained from Kurary Co. Ltd., Kurashiki, Japan, which was used after hydrolysis in 0.1 M NaOH at 60 °C for 5 h. *N*-succinimidyl polyethylene glycol with a mean molecular weight of 2300 containing ester bond between PEG and N-succimide was obtained from NOF, Tokyo, Japan. RPMI-1640 medium and fetal bovine serum was obtained from GIBCO, Grand Island, NY. Primary antibody against human heme oxygenase-1 (HO-1) was obtained from Santa Cruz Biotechnology, Inc., CA. FITC-labeled goat anti-rabbit IgG labeled with FITC was obtained from Biomedical Technologies, Inc., MA. Ethylenediamine and other chemicals were reagent grade commercially available.

2.2. Synthesis of ZnPP and SMA-ZnPP

ZnPP and SMA-ZnPP was prepared according to the method as described by Iyer et al. previously [11]. Briefly hydrolysed SMA (cSMA) was dissolved at concentration of 10 mg/ml in deionized water and pH was adjusted to 10.5 with 0.1 M NaOH. ZnPP solution at 5 mg/ml in DMSO was added to cSMA solution under stirring for 1 h. Then the pH was adjusted slowly to pH 3.0 using 0.1 M HCl at 20 °C resulting in precipitation of SMA-ZnPP micelles. Precipitates were collected by centrifugation and were washed with cold deionized water thrice. The precipitates were resuspended in deionized water and pH was adjusted to 7.4 with 0.1 M NaOH to obtain clear solution of SMA-ZnPP. Finally ultrafiltration using the Millipore Lab Scale TFF system (Millipore, Bedford, MA) with a membrane cut-off MW of 10 kDa under a pressure of about 0.7 kg/cm^2 was carried out to remove low MW components including excess free cSMA and concentrate the SMA-ZnPP micelles to 1/10 volume, of which process was repeated three times at 4 °C. Then, the concentrate was lyophilized to obtain fluffy deep brownish powder. Finally obtained SMA-ZnPP contains 35 w/w% of ZnPP in its micellar structure.

2.3. Synthesis of PEG-ZnPP

PEG-ZnPP micelles were prepared according to the method described by Sahoo et al. with some modification [9]. Briefly carboxyl group of PP (100 mg in 20 mL of tetrahydrofran) was reacted with ethylenediamine (2.4 mL) to introduce two functional amino groups via amide bond to PP. The obtained product, *bis*-(diaminoethyl) protoporphyrin (PPED) was absorbed onto the activated alumina and washed with chloroform five times. Then PPED was eluted with chloroform containing 5% ethylenediamine. And then polyethylene glycol (mean Mw of 2300) with succinimide (54 mg) was reacted to PPED (5 mg). Obtained pegylated protoporphyrin (PEG-PP) was applied to aluminum oxide column (2.5 cm × 10 cm) equilibrated with chloroform and eluted with chloroform to remove unreacted PPED. Then 100 M excess of zinc acetate was added to PEG-PP with stirring and zinc was chelated for 2 h to achieve PEG-ZnPP. PEG-ZnPP was transferred to water followed by Amicon® ultra filtration system with 10 kDa cut off membrane under pressure condition (0.2 MPa) to remove unreacted PEG and excess zinc acetate. Product showed a single peak on HPLC using column of Asahipack GF310-HQ (solvent system: 70% methanol, 30% DMSO and 0.001% trifluoroacetic acid).

2.4. Cell culture

Human chronic myeloid leukemia cell lines (K562) were cultured in RPMI 1640 with 10% fetal bovine serum at 37 °C under the atmosphere of 5% CO_2-95% air.

2.5. Quantification of ZnPP in cells

K562 cells were placed in 12-well plate (5×10^5 cells/well). After overnight pre-incubation, cells were treated with ZnPP, SMA-ZnPP or PEG-ZnPP for indicated time at the concentrations shown in the figure legend. Free ZnPP was dissolved in DMSO, other micellar ZnPP was dissolved in PBS (pH 7.4). After incubation for given times, cells were collected by centrifugation and washed with PBS thrice at 4 °C. Then cells were sonicated (30 W, 30 s, Dr.Hielscher, UP50H homogenizer, tip drip type) in ethanol at ice chilled condition (0 °C) followed by centrifugation to collect supernatant containing ZnPP, and fluorescence intensity (excitation at 420 nm, emission at 598 nm) of the ethanol extract was measured.

2.6. Subcellular localization of ZnPP micelles

Subcellular localization of SMA-ZnPP was analyzed by Nikon Eclipse TE2000-E Confocal Microscope (Nikon, Japan). K562 cells were cultured in RPMI medium with 10% FCS without phenol red in 35 mm (Ø) glass bottom dish (Matsunami glass, Osaka, Japan). Cells were treated with 30 μM of ZnPP, SMA-ZnPP or PEG ZnPP for indicated time at 4 °C or 37 °C. ZnPP, SMA-ZnPP and PEG-ZnPP were excited by 488 nm and detected through the 565–615 nm band path filter. To investigate the colocalization of ZnPP derivatives at ER compartment, 3,3′-dihexyloxacarbocyanine iodide (DIOC6) was used for a staining of ER (endoplasmic reticulum). DIOC6 was excited at 488 nm and detected through the 500–530 nm band path filter. In this experiment, ZnPP and SMA-ZnPP were excited at 543 nm and were visualized by 565–615 nm band path filter to avoid a bleed from a fluorescence of DIOC6.

2.7. Immunofluorescence staining

K562 cells treated with ZnPP or SMA-ZnPP for 3 h were collected by centrifugation (1000 rpm, 5 min, 4 °C) and washed with PBS thrice. The cells were fixed with 4% paraformaldehyde at room temperature for 10 min following washing twice with PBS containing 10 mM glycine. Then the cells were made permeable with 0.1% Triton X-100 for 10 min at room temperature and washed with PBS thrice, followed by treatment with 3% BSA in PBS at room temperature for 30 min to react excess remaining paraformaldehyde and then washed thrice for 5 min in PBS. The cells were then incubated with primary rabbit antibody against human HO-1 (diluted 1:100 in 3% BSA) at room temperature for 1 h. After washing with PBS thrice, the cells were incubated with FITC-labeled goat anti-rabbit IgG (diluted 1:1000) at 25 °C for 1 h and then again washed thrice for 10 min in PBS. Then cells were resuspended in PBS, and examined under a confocal microscope. Both FITC-labeled goat anti-rabbit IgG and ZnPP was excited at 488 nm and detected through a 485–530 nm band path filter and a 565–615 nm band path filter respectively.

2.8. Analysis of mechanism of intracellular uptake of ZnPP micells into cells

The cells were seeded in 12-well culture plates at a density of 2×10^5 per well, and incubated at 4 °C, or at 37 °C for indicated time period with or without various inhibitors of endocytosis for 1 h prior to the addition of ZnPP, SMA-ZnPP or PEG-ZnPP. After incubation, the cells were harvested by centrifugation at 700 rpm and washed with PBS thrice at room temperature followed immediately by flow cytometry analysis (FACSCalibur, Becton Dickinson and Co.). About 1×10^4 cells were collected, and the mean fluorescence intensity was recorded and analyzed for each sample.

2.9. Disintegration study of SMA-ZnPP in cell free system

SMA-ZnPP micelle (4 μg/mL) was incubated with sodium dodecyl sulfate, soybean lecithin (wako) or rat liver microsome fraction at 25 °C. Disintegration of SMA-ZnPP was also examined in 50 mM phosphate buffer (pH7.5) or 20 mM citrate buffer (pH5.0) with 150 μg/mL of lecithin. At the indicated time period, incubates were excited at 420 nm and fluorescent intensity at 599 nm was measured by fluorescent spectrometer.

2.10. HPLC analysis of intracellular PEG-ZnPP and HO-1 inhibitory assay

K562 cells were treated with 30 μM of PEG-ZnPP for 5 h, and then cells were washed with PBS thrice, followed by extraction of intracellular PEG-ZnPP with ethanol. The extracted PEG-ZnPP was then subjected to HPLC analyses with an Asahipak GF-310 HQ column (7.5 mm × 300 mm). The mobile phase consisted of 70% methanol, 30% dimethyl sulfoxide and 0.001% of trifluoroacetic acid at a flow-rate of 0.8 mL/min. Elutes was detected at 415 nm of ZnPP. HO-1 inhibitory activity of PEG-ZnPP was performed as described previously [9]. Briefly, PEG-ZnPP derivatives were incubated with rat liver cytosolic fraction (1.0 mg/mL of protein) in 100 mM phosphate buffer (pH7.4) for 30 min at 25 °C. Then rat splenic microsomal fraction (1.0 mg/mL of protein), 333 μM nicotinamide adenine dinucleotide phosphate (NADPH) and 33 μM of hemin was added to initiate the reaction. The reaction mixture was incubated for 30 min at 37 °C. The bilirubin formed in the reaction was extracted with 1.0 mL of chloroform, and the bilirubin concentration was determined spectroscopically by the difference in absorbance at 465 nm and 530 nm.

3. Result

3.1. Intracellular behavior of SMA-ZnPP and PEG-ZnPP

Protoporphyrin IX (PP) itself does not inhibit HO-1 enzymatic activity, however, the zinc coordination with protoporphyrin IX (ZnPP) becomes inhibitor for HO-1 activity. The Ki value is almost the same among ZnPP, SMA-ZnPP and PEG-ZnPP [9,11]. Protoporphyrin IX has an absorption max (λ_{max}) of 406 nm and exhibit single fluorescence emission peak at 641.5 nm in ethanol, while that of authentic ZnPP has λ_{max} 422.5 nm and fluorescent max at 598.5 nm with a minor shoulder approximately at 650 nm in ethanol. To quantify the ZnPP derivatives in the cells, it was extracted by 95% ethanol and fluorescent spectrum was examined. As shown in Fig. 2, intracellular ZnPP showed fluorescence emission peak at 598.5 nm which is consistent with that of authentic ZnPP. SMA-ZnPP and PEG-ZnPP also showed fluorescent spectrum which is consistent to that of ZnPP.

3.2. Intracellular uptake and subcellular localization of ZnPP micelles

Fluorescent intensity of ZnPP derivatives will change by its conformational states. In water solution, both ZnPP derivatives form micellar structure and its fluorescence is quenched. Its fluorescence is recovered by addition of EtOH (Fig. 3a). However its fluorescence quenching of PEG-ZnPP in water solution is weaker than that of SMA-ZnPP, probably due to the different micellar structure of these two compounds. To quantify the amount of ZnPP derivatives by fluorescent intensity, we checked fluorescent efficiency of ZnPP, SMA-ZnPP and PEG-ZnPP in ethanol, in which all micelles are disrupted and emit fluorescence. The concentration of ZnPP derivatives was standardized as ZnPP equivalent concentration by absorbance at 420 nm. Three ZnPP derivatives showed comparable fluorescent intensity under micelle disrupting condition in ethanol (Fig. 3b). To examine the cellular

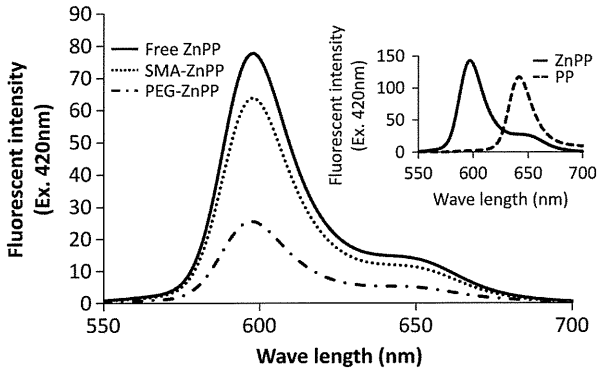

Fig. 2. Fluorescent spectra of ZnPP (solid line), SMA-ZnPP (dashed line) and PEG-ZnPP (dash–dot line) of extracts from the treated cells. K562 cells were treated with 20 μM of ZnPP, SMA-ZnPP and PEG-ZnPP for 5 h. After incubation, fluorescent spectra of intracellular ZnPP, SMA-ZnPP and PEG-ZnPP were recorded as described in Materials and methods. Inset shows the fluorescent spectra of protoporphyrin IX (PP) (dashed line) and ZnPP (solid line) in ethanol.

internalization of ZnPP and both types of ZnPP micelles, K562 cells were incubated with them for indicated time. Intracellular ZnPP was extracted with ethanol and quantified by fluorescence intensity of ZnPP itself (Ex. 420 nm and Em. 590 nm). As shown in Fig. 3, ZnPP and both ZnPP micelles were incorporated into the cells in a time dependent manner. More interestingly, uptake of SMA-ZnPP into the cells was about 2.5 times more efficiently than PEG-ZnPP at 300 min incubation.

Intracellular localization of ZnPP and ZnPP micelles were also examined under the fluorescent confocal laser microscopy. Confocal laser microscopy imaging showed that ZnPP and both ZnPP micelles accumulated at the cellular membrane at first and then gradually accumulated more distinctly at the perinuclear site after 30 min or later (Fig. 4). ZnPP is highly hydrophobic and is predicted to be associated with hydrophobic compartment in the cell. Thus we first examined the possibility of localization of free ZnPP and SMA-ZnPP micelles at the endoplasmic reticulum (ER); for that purpose we performed double staining with a DIOC6 which accumulates in the ER and emits fluorescence at the ER (Fig. 5a). As shown in Fig. 5a, ZnPP and both ZnPP micelles colocalized with DIOC6 suggesting localization of free ZnPP and ZnPP micelles in the ER. Because heme oxygenase-1 (HO-1) is found mainly at the ER as stained with antibody against HO-1, we hypothesized that ZnPP and SMA-ZnPP colocalized with HO-1. As expected, ZnPP and SMA-ZnPP showed clear colocalization with HO-1 protein when ZnPP or SMA-ZnPP was added to K562 cells (Fig. 5b).

3.3. Mode of intracellular uptake of ZnPP and ZnPP micelles; endocytosis

To evaluate the mechanism of intracellular uptake of ZnPP and ZnPP micelles, K562 cells were incubated with 20 μM each of ZnPP, SMA-ZnPP and PEG-ZnPP respectively at 4 °C or 37 °C for 2 h. As shown in Fig. 6, ZnPP and ZnPP micelles were taken up into the cells efficiently at 37 °C during incubation, however, intracellular uptake of free ZnPP and SMA-ZnPP micelles were suppressed to a great extent at 4 °C as revealed by FACS analysis (Fig. 6b). Further, compared to the strong staining of ZnPP, SMA-ZnPP or PEG-ZnPP micelles in cells at 37 °C, they showed no or quite faint staining only at a cellular membrane when incubated at 4 °C (Fig. 6). In addition, as shown in Fig. 7, internalization of ZnPP was inhibited by macropinocytosis

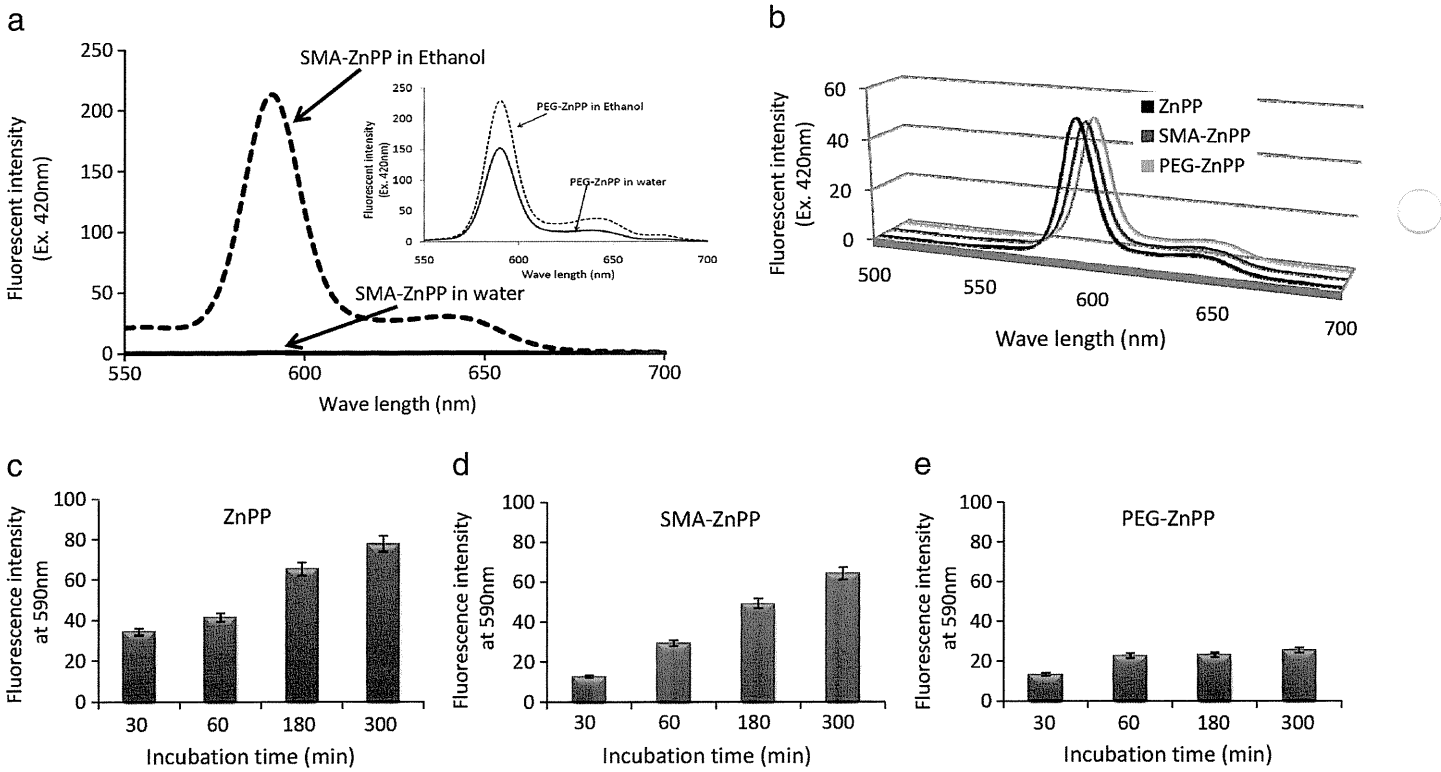

Fig. 3. Intracellular uptake of ZnPP derivatives as quantified by fluorescence intensity after extraction of ZnPP. (a) SMA-ZnPP (4 μg/mL) or PEG-ZnPP (14ug/mL) was dissolved in distilled water or ethanol, which was excited at 420 nm and fluorescent spectrum was recorded by fluorescent spectrometer. (b) 0.25 μM ZnPP equivalent of ZnPP, SMA-ZnPP and PEG-ZnPP in ethanol was excited at 422 nm and fluorescent spectra were recorded. K562 cells in suspension culture were treated with 20 μM of (c) free ZnPP, (d) SMA-ZnPP and (e) PEG-ZnPP for period of indicated time. After incubation, the cells were washed with PBS and the amount of intracellular ZnPP and SMA-ZnPP and PEG-ZnPP were determined after extraction by ethanol as described in Materials and methods.

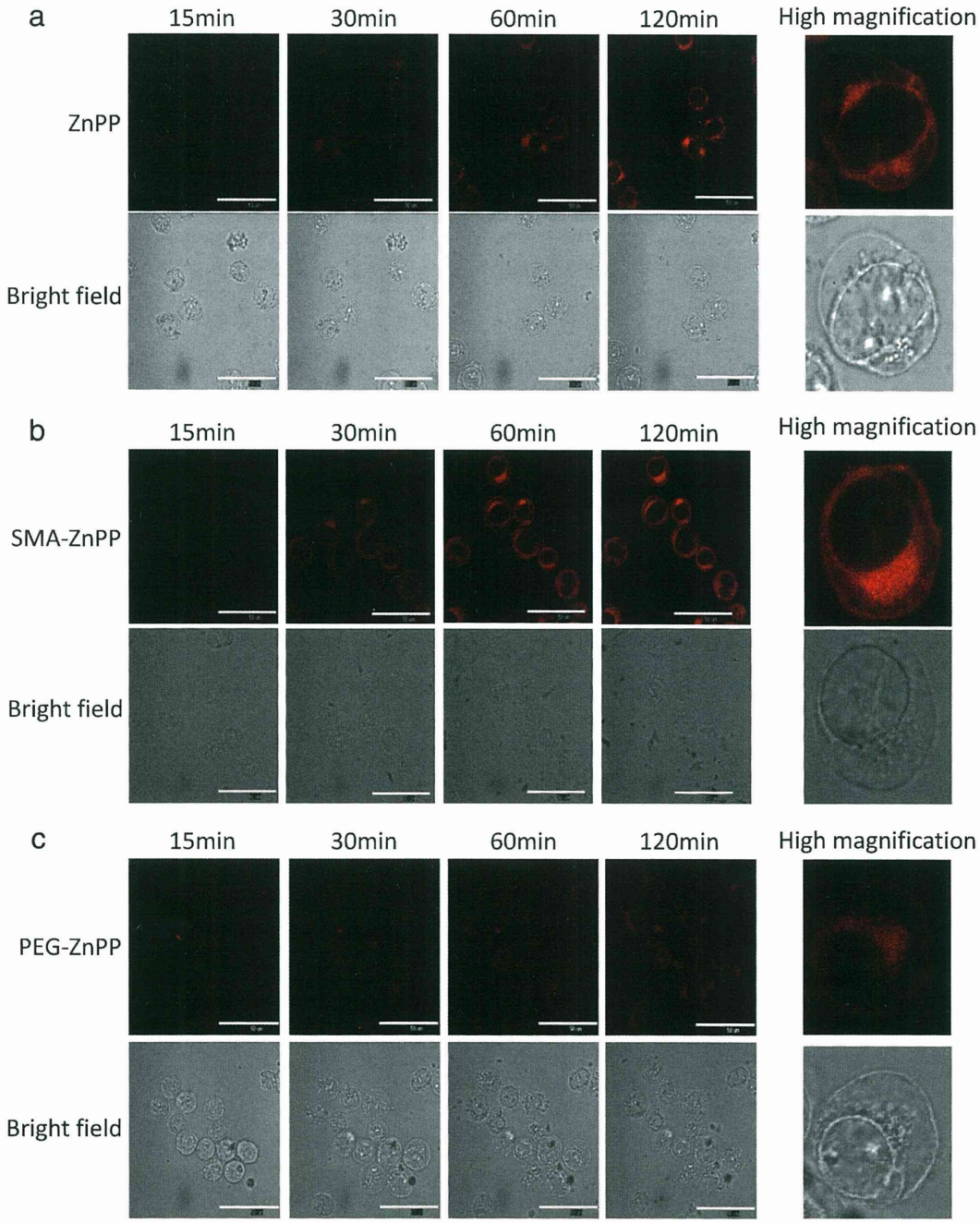

Fig. 4. Confocal fluorescence microscopy of K562 cells treated with 30 μM of (a) ZnPP, (b) SMA-ZnPP and (c) PEG-ZnPP. K562 cells were grown on glass bottom dish to logarithmic phase, incubated with 30 μM of ZnPP, SMA-ZnPP and PEG-ZnPP at 37 °C for indicated time. Cells were then taken for microscopic observation. Red color indicates the fluorescence of ZnPP. Scale bar shows 50 μm length.

inhibitor, amiloride. Pretreatment with sucrose and colchicine suppressed uptake of SMA-ZnPP, similarly intracellular uptake of PEG-ZnPP was suppressed by sucrose treatment (Fig. 7).

3.4. Disintegration of SMA-ZnPP micelles by amphiphilic components of cells

In the SMA-ZnPP micelles, SMA is thought to form a shell of micelle where ZnPP is encapsulated inside of the micelles, which is believed to be liberated eventually for its action. Therefore, disruption of SMA-ZnPP micelles followed by liberation of ZnPP is a crucial step to exert the pharmacological effect to inhibit HO-1 enzyme activity in the cells. To examine this possibility of disruption of SMA-ZnPP micelles in cells, we carried out a model experiment, in that SMA-ZnPP was incubated with soybean lecithin which mimics the cellular membrane components, phosphatidylcholine. As shown in Fig. 8, SMA-ZnPP does not emit fluorescence in water solution and exhibits fluorescence when ZnPP is liberated from the micelles as disrupted by ethanol or 10% SDS [11]. Coincubation with increasing amount of lecithin or SDS indeed resulted in increased fluorescence emission from free ZnPP. Vehicle alone has no effect on fluorescence increament of SZP (Fig. 8a). Time dependent increase of fluorescence emission was also seen when incubated with soybean lecithin. Fig. 8b also shows that SMA micelle disruption with lecithin proceeds rapidly at the condition of pH 7.5 than pH 5.5. Similar results were obtained when it was incubated with mouse liver microsomal fraction which contains membrane components (Fig. 8c).